NASA Contractor Report 191541

ICASE Report No. 93-72

ICASE

CONVECTION EFFECTS ON RADIAL SEGREGATION AND CRYSTAL MELT INTERFACE IN VERTICAL BRIDGMAN GROWTH

S. Tanveer

NASA Contract Nos. NAS1-18605 and NAS1-19480
September 1993

Institute for Computer Applications in Science and Engineering
NASA Langley Research Center
Hampton, Virginia 23681-0001

Operated by the Universities Space Research Association

National Aeronautics and
Space Administration

Langley Research Center
Hampton, Virginia 23681-0001

ICASE Fluid Mechanics

Due to increasing research being conducted at ICASE in the field of fluid mechanics, future ICASE reports in this area of research will be printed with a green cover. Applied and numerical mathematics reports will have the familiar blue cover, while computer science reports will have yellow covers. In all other aspects the reports will remain the same; in particular, they will continue to be submitted to the appropriate journals or conferences for formal publication.

CONVECTION EFFECTS ON RADIAL SEGREGATION AND CRYSTAL MELT INTERFACE IN VERTICAL BRIDGMAN GROWTH

S. Tanveer[1]
Mathematics Department
Ohio State University
Columbus, OH 43210

ABSTRACT

We analytically study the influence of convection caused by horizontal heat transfer through the sides of a vertical Bridgman apparatus. We consider the case when the heat transfer across the side walls is small so that the resulting interfacial deformation and fluid velocities are also small. This allows us to linearize the Navier-Stokes equations and express the interfacial conditions about a planar interface through a Taylor expansion. Using a no tangential stress conditions on the side walls, asymptotic expressions for both the interfacial slope and radial segregation at the crystal-melt interface are obtained in closed form in the limit of large thermal Rayleigh number. It is suggested that these can be reduced by appropriately controlling a specific heat transfer property at the edge of the insulation zone in the solid side.

[1]This research was supported by the National Aeronautics and Space Administration under NASA Contract Nos. NAS1-18605 and NAS1-19480 while the author was in residence at the Institute for Computer Applications in Science and Engineering (ICASE), NASA Langley Research Center, Hampton, VA 23681. Additional support was received from the National Science Foundation (NSF DMS-9107608) and NASA (NAG3-1415).

1 Introduction

In a vertical Bridgman apparatus, a cylindrical container (Fig. 1) containing a melt of a binary alloy mixture is translated downwards from a hot to a cold zone so as to cause solidification. The uniformity of composition of the resulting crystal and the relative absence of crystal defects are desirable features for technological applications. Ideally, these can be achieved if convection is eliminated and the crystal-melt interface is planar. However, in practice, this is difficult to ensure. Considerations of constitutional supercooling (morphological instability) and the need to avoid transient effects due to container ends require a relatively large temperature gradient. On the other hand, a completely one dimensional imposed temperature gradient that would occur (Tiller et al[1]) when the cylinder sides are insulated would require unrealistic large temperature differences between the two cylinder ends given that the length of the cylinder has to be large enough to avoid transient effects. Thus, one is forced to a configuration where significant heat flux occurs through the cylinder sides. However, when this happens, fluid next to the cylinder ends is hotter than the fluid at the center leading to convection for any value of the solutal or thermal Rayleigh number. The review by Brown[2] discusses the Bridgman problem in great detail. Other review papers[3–5] deal with various aspects of directional solidification in general.

There are many papers in the literature that address the problem of onset of convection in finite and infinite geometries (see references 6-15 and references there in). In these cases, the equations allow for a basic quiescent state (no fluid flow) that is stable upto a certain critical Rayleigh number. Such convection can be termed natural convection, as opposed to the induced convection caused by heat transfer through the side walls of a Bridgman apparatus. Since this paper concerns situations which in the absence of horizontal heat transfer is a thermally stable configuration, natural convection is not relevant in this context unlike that of an otherwise thermally or solutally unstable arrangement where possibility exists of a "resonant" response leading to vigorous convection.

There are many papers dealing with the Bridgman problem itself (see Brown, 1988 for references). Nonetheless, the first set of fully consistent calculations that account for convection in the fluid, and its coupling with thermo-solutal field, heat diffusion in the solid and a non-planar interface appear to be due to Chang & Brown[16] and Adornato & Brown[17]. By assuming a quasi-steady growth when the transient scale is small, they calculate the nonlinear steady states numerically. Later on, these calculations were further extended by Kim & Brown[18] by including effects of heat transfer through an ampoule that surrounds the cylinder in an experiment. Unsteady transient effects have also been studied by Brown & Kim[19] and these calculations are in good agreement with experiment. These calculations

suggest among other things that the classic one-dimensional modelling through the Scheil equation[20] is an oversimplification since it assumes complete and through mixing all over the fluid. It is known for instance that between the diffusive limit, where convection can be totally neglected and the thoroughly mixed limit for which Scheil's equation applies, there is an imperfect mixing zone at moderately large Rayleigh number. In this range, radial segregation and the interface deformation are larger than at very large Rayleigh number. Indeed, it was pointed out that reduction of gravity by a factor of $10^3 - 10^4$ compared to earth may be detrimental to growing a crystal of uniform composition. Despite such advances in theoretical understanding, it is difficult from numerical results alone to get a global understanding of the parameter dependences since there are so many of them (See Table 1). The trends in a certain subset of parameter space need not reflect the trend in other ranges of the parameter space. Thus, there is need for analytical results, which is likely to be of limited validity; nonetheless it can be complimentary to numerical calculations.

The only analytical work that we are aware of that is relevant to convection in the Bridgman apparatus is due to Brattkus & Davis[21]. They analyzed a two dimensional model where the vertical dimension is far larger than the horizontal dimension and the heat flux through the side walls is assumed small. Brattkus & Davis[21] specifically concluded there was no necessary relation between radial segregation and interfacial shape, a hypothesis put forward by Coriell & Sererka[22] based on diffusion alone. The numerical results of Brown and his coworkers, on the other hand, suggests a strong correlation between the two. However, the Brattkus-Davis analysis ignores the insulation zone shown in Figure 1. This insulation zone length is known to be an important parameter from prior numerical work (see Chang & Brown[16], for instance).

Here we consider steady state[2] inside a vertical cylinder (Figure 1) between $z = 0$ and $z = z_2$, where z_2 is assumed a constant. As in Brattkus & Davis[21], the horizontal heat transfer is assumed small enough so that both the fluid velocities and the interfacial deformation are small. Prior numerical work (Chang & Brown[16] for instance) show that the latter assumption is valid even for relatively intense convection. The fluid velocity on the other hand has to be small so that nonlinearities in Navier-Stokes equation can be ignored. This assumption is clearly unrealistic in many experimental situations; however, as discussed in section 7, there are reasons to believe that the results on radial segregation and interfacial deformation will hold in part of the nonlinear regime as well.

The above assumptions allow us to linearize about a basic one dimensional state and Taylor expand the interfacial boundary conditions about the original planar boundary. By

[2]In reality, this is a quasi-steady state (see Brown (1988)); however for purposes of this paper, we make no such distinction.

modifying the no-slip boundary condition at the cylinder side walls, we find a modal representation for each of the stream function, radial temperature and concentration gradient in the melt that decouples each modes and reduces the problem to a set of finite ordinary differential equations for each mode. By making use of general expressions for the perturbed temperature and concentration fields in the solid, we find that the interfacial conditions can be expressed in terms of effective boundary conditions on the melt variables at the original planar interface. With the effective boundary conditions on a planar interface, we solve the linearized melt equations and find explicit expressions for interfacial deformation and radial segregation in the asymptotic limit of large thermal Rayleigh number R_T. Among other things, we find that there is a boundary layer near the interface that scales as $R_T^{-1/6}$, where each of the solutal, thermal and fluid velocity field change rapidly. The radial derivative of the temperature field and the radial segregation in the crystal, each scale as $R_T^{-1/6}$, provided $|R_c| << R_T^{5/6}$. The coefficient of $R_T^{-1/6}$ in each scale decreases exponentially with the distance of the interface from the end of the insulation zone in the solid side. In a certain range of parameters, consistent with many experimental conditions, our results suggest that radial dependence of the interface shape and concentration will be roughly given by the Bessel function $J_0(\lambda_1 r)$, where λ_1 is the first positive root of $J_0'(\lambda_n) = 0$ (i.e. zero of J_1). Further, we find that in this case, the Coriell-Sererka (Coriell & Sererka[22]) hypothesis of proportionality between interface slope and radial segregation is approximately valid, though the constant of proportionality is different from what these authors find with diffusion only. In this case, we also point out a specific condition on heat transfer near the solid end of the insulation zone, which when satisfied, will result in minimal interfacial slope and radial segregation for large R_T.

2 Mathematical Model

In a Bridgman apparatus (Fig. 1), a binary melt is contained in a cylindrical container of radius a that is translated downwards with constant velocity $-U_a\,\hat{z}$, where $\hat{z}$ is a unit vector along the axis of the cylinder that opposes gravity, as shown in Figure 1. The concentration of solute (one of the two components of the binary mixture) at the top of the cylinder $\tilde{z} = \tilde{z}_2$ is $c = c_2$. The top of the cylinder is maintained at temperature $\tilde{T} = \tilde{T}_2$, while the bottom of the cylinder is at temperature $\tilde{T} = \tilde{T}_1$, which is significantly smaller than the melting temperature $\tilde{T}_0$ of a planar interface. The density of the melt is assumed to be $\tilde{\rho} = \tilde{\rho}_0$ at temperature $\tilde{T}_0$ and concentration c_2. This will be the reference density. We scale all lengths by a, all time scales by a/U_a, all mass scales by $\tilde{\rho}_0 a^3$ and all temperatures by $\tilde{T}_2 - \tilde{T}_0$, leaving us with non-dimensional quantities of Table 1. Concentration will remain

unscaled, as it is already nondimensional. Given the fair amount of algebraic manipulation, we prefer to use this set of parameters as it keeps the equations looking simpler. Off course, in the common Engineering literature, it is common to express these quantities in terms of Peclet number Pe, Reynolds number Re, Prandtl number Pr, etc. For the benefit of the readers, we have prepared Table 2 that expresses our non-standard parameters in terms of the more well-known dimensionless numbers. In section 7, we also discuss our results using the more standard notation to benefit the reader who is more interested in the concrete results than in the analysis.

Using the nondimensional variables in Table 1, the top end of the cylinder, corresponding to $z = z_2$, is maintained at nondimensional temperature $T = 1$ and the bottom end is maintained at temperature T_1 with $T_1 < 0$. The temperature gradient is assumed strong enough to avoid constitutional supercooling. The heat is allowed to flow through the sides of a cylinder for $z_2 > z > z_{II}$ in the melt zone and $0 < z < z_I$ in the crystallized zone. The heat transfer across the side walls is such that the fluid velocities are slow and the interface deformation from a planar interface is small. The precise limitations placed on the size of the heat transfer by this assumption will be examined later in section 6. For the present, it suffices to assume that heat transfer is sufficiently small. We introduce a cylindrical coordinate system (r, z) where r is the radial direction. No azimuthal angular variable is necessary as the flow variables are assumed to be axi-symmetric. The mathematical equations for the steady solution in the melt are

$$\vec{v} \cdot \nabla T = \kappa \nabla^2 T, \tag{1}$$

$$\vec{v} \cdot \nabla c = D \nabla^2 c, \tag{2}$$

$$\vec{v} \cdot \nabla \vec{v} = -\nabla p + \{\alpha T + \beta (c - c_2)\} g \hat{z} + \nu \nabla^2 \vec{v}, \tag{3}$$

$$\nabla \cdot \vec{v} = 0, \tag{4}$$

where T denotes the nondimensional temperature, c the concentration of solute (one of the components) relative to the total (measured in molar fraction) and $\vec{v}$ is the relative melt velocity (see Table 1) and ν denotes the nondimensional kinematic viscosity (i.e inverse Reynolds number based on U_a). In equations (3) and (4), we have invoked the usual Boussinesq approximation, where the density variation due to change in temperature and concentration from reference values are included only in the forcing term on the right hand side of (3). Here, α (> 0) and β are the non-dimensional coefficients of volumetric expansion due to increased T and c respectively. When the solute density is smaller than the alloy, $\beta > 0$. However, there is no restriction on the sign of β in our current analysis.

On the crystal side, since there is no fluid motion and so

$$\vec{v} \;=\; -\,\hat{z}. \tag{5}$$

Thus the equations for temperature and concentration fields are given by

$$-\,\frac{\partial\, T_s}{\partial z} \;=\; \kappa_s\, \nabla^2\, T_s, \tag{6}$$

$$-\,\frac{\partial\, c_s}{\partial z} \;=\; D_s\, \nabla^2\, c_s. \tag{7}$$

Now comes the boundary conditions. Denoting the r and z components of $\vec{v}$ by (u, w), we take the boundary condition on fluid velocity components at the sidewalls $r \;=\; 1$ as

$$u \;=\; 0, \tag{8}$$

$$\frac{\partial w}{\partial r} \;=\; 0. \tag{9}$$

Equation (9) is a no-stress condition. A no slip condition $w = -1$ would be more realistic; however, we could find no simple basis representation of the solution in this case. We suspect that aside from the changing the nature of a boundary layer near $r = 1$, the change of this boundary condition will be have no global effect on crystal shape and radial segregation, at least in the li· it of large Rayleigh number.

The condition of no mass flux through the side walls imply

$$\frac{\partial c}{\partial r} \;=\; 0. \tag{10}$$

Also, the condition of heat flux imply

$$\frac{\partial T}{\partial r} \;=\; 0 \quad \text{for} \quad f(1) \;<\; z \;<\; z_{II}, \tag{11a}$$

$$\frac{\partial T}{\partial r} \;+\; \epsilon\, q_1\, T \;=\; \epsilon\, q_2 \quad \text{for} \quad z_{II} \;<\; z \;<\; z_2. \tag{11b}$$

On the solid side, at $r \;=\; 1$,

$$\frac{\partial c_s}{\partial r} \;=\; 0, \tag{12}$$

$$\frac{\partial T_s}{\partial r} \;=\; 0 \quad \text{for} \quad f(r) \;>\; z \;>\; z_I, \tag{13a}$$

while

$$\frac{\partial T_s}{\partial r} \;+\; \epsilon\, q_{1s}\, T_s \;=\; \epsilon\, q_{2s} \quad \text{for} \quad z_I \;>\; z \;>\; 0. \tag{13b}$$

Each of ϵq_1 , ϵq_2 , ϵq_{1s} and ϵq_{2s} will be taken as constants that characterize the heat transfer through the side walls. In the common engineering literature, ϵq_1 and ϵq_{1s} are

Biot numbers related to heat transfer through the side walls in the melt and solid region respectively. For instance, in equation (16) of the Adornato & Brown[17] paper, the notation $Bi(z)$ with a specific choice of a piecewise constant profile, is related to the constants ϵq_{1_s} and ϵq_1, while $Bi(z)\theta_\infty(z)$ is related to ϵq_{2_s} and ϵq_{2_s}, provided we ignore the ampoule in their model. The quantity ϵ will be assumed small, while each of q_1 and q_2 assumed $O(1)$. ϵ will be our perturbation parameter. The precise multiplicative decomposition of the Biot number ϵq_1 into q_1 and ϵ is unimportant since in the final results, only the product ϵq_1 appears. The same is true for ϵq_2 , ϵq_{1_s} and ϵq_{2_s}.

At the cylinder top, i.e. $z = z_2$, we have the nondimensional temperature

$$T = 1, \tag{14}$$

$$c = c_2, \tag{15}$$

$$u = 0, \tag{16}$$

$$w = -1, \tag{17}$$

with c_2 being assumed a constant. Similarly at the bottom, $z = 0$, we get

$$T_s = T_1, \tag{18}$$

$$c_s = c_2, \tag{19}$$

where $T_1 < 0$ and assumed smaller than the nondimensional melting temperature at the interface. Note that one can use more general boundary conditions than (19), however this appears to be most relevant since in the limit of an infinitely long cylinder, conservation of mass dictates that the concentration should be the same at $z = \pm\infty$.

Now comes the boundary conditions on the solid melt interface $z = f(r)$. We will assume local thermodynamic equilibrium since the relaxation time of the departure from equilibrium can safely be assumed to be much smaller than the typical time scales in this problem. Thus, at the interface, we satisfy the melting condition given by the solidus-liquidus line with the incorporation of the Gibbs-Thompson effect (i.e. lowering of the melting temperature in the presence of curvature effects)

$$T = T_s = -m\,c + d_0 \left\{ \frac{f''}{(1 + f'^2)^{3/2}} + \frac{1}{r}\,\frac{f'}{(1 + f'^2)^{1/2}} \right\}. \tag{20}$$

Further, from the solidus liquidus line, we must have

$$c_s = k\,c. \tag{21}$$

The continuity of heat flow implies that

$$T\,\vec{v}\cdot\hat{n} \;-\; \kappa\,\frac{\partial T}{\partial n} \;=\; -T_s\,\hat{z}\cdot\hat{n} \;-\; \kappa_s\,\frac{\partial T_s}{\partial n} + S_t\,\vec{v}\cdot\hat{n}, \tag{22}$$

where $\hat{n}$ denotes a unit vector normal to the melt-solid interface pointing towards the liquid, and $\frac{\partial}{\partial n}$ denotes component of gradient in that direction, S_t is the nondimensional latent heat (Stefan number). From the conservation of solute concentration across the interface, we must have

$$c\,\vec{v}\cdot\hat{n} \;-\; D\,\frac{\partial c}{\partial n} \;=\; -c_s\,\hat{z}\cdot\hat{n} \;-\; D_s\,\frac{\partial c_s}{\partial n}. \tag{23}$$

Further, from integrating (4) over a small control volume centered about a point on the interface, it follows that normal velocity is continuous when the difference of densities between the melt and the crystal is neglected. Thus,

$$\vec{v}\cdot\hat{n} \;=\; -\,\hat{z}\cdot\hat{n}. \tag{24}$$

Difference of densities between solid and liquid side of the interface can be accommodated by including an additional $-\frac{(\rho_s-\rho)}{\rho}\hat{z}\cdot\hat{n}$ term on the right hand side of (24); however, here we will be primarily interested in situations where this is not important. Further, at the interface, if we assume a no-slip condition for the fluid flow relative to the solid, then

$$u + (w+1)f' = 0. \tag{25}$$

While the no-slip condition (25) at the melt-solid interface seems to be widely used in the literature, we are unaware of any convincing physical argument this is superior to a no tangential stress boundary condition. It may be pointed out that unlike the case of a fluid next to a solid where good experimental evidence exists for the no-slip boundary condition, the liquid molecules in this case do not preserve their identity as it goes through a phase transition. Nonetheless, despite this uncertainty, we find that the asymptotic scalings and parameter dependence presented later in this paper remain the same with a no-stress boundary condition, only the scaling constants differ.

Note that the mathematical model with equations (1)-(4), (6), (7) and boundary and interfacial conditions (8)-(25) contain twenty irreducible nondimensional parameters D, D_s, κ, κ_s, αg, βg, ν, z_2, z_I, z_{II}, ϵq_1, ϵq_{1_s}, ϵq_2, ϵq_{2_s}, c_2, T_1, d_0, m, k and S_t. The relation of the less standard parameters in this list with the conventional Peclet number, Prandtl number, Reynolds number, etc. is given in Table 2.

3 Steady state for zero epsilon

Despite the complexity of the general equations, there exists well known simple solutions to the above equations, as determined originally by Tiller et al[1]. If $\epsilon = 0$, a quiescent state

is a simple solution to the above equations in which the melt velocity $\vec{v} = -\hat{z}$ and the melt-solid interface is planar, i.e. $f = z_0$, a constant. The temperature and concentration fields in this case are denoted by a superscript 0 as they are the leading term of an expansion for small ϵ. They are given by

$$T^0 = T_i + \left(e^{-\frac{(z-z_0)}{\kappa}} - 1\right) \frac{1 - T_i}{e^{-\frac{1}{\kappa}(z_2-z_0)} - 1}, \tag{26}$$

$$c^0 = c_i + \left(e^{-\frac{1}{D}(z-z_0)} - 1\right) \frac{c_2 - c_i}{e^{-\frac{1}{D}(z_2-z_0)} - 1}. \tag{27}$$

On the solid side, $z_0 > z > 0$,

$$T_s^0 = T_i + \left(e^{-\frac{1}{\kappa_s}(z-z_0)} - 1\right) \frac{T_1 - T_i}{e^{\frac{1}{\kappa_s}z_0} - 1}, \tag{28}$$

$$c_s^0 = k\, c_i + \left(e^{-\frac{1}{D_s}(z-z_0)} - 1\right) \frac{c_2 - k\, c_i}{e^{\frac{1}{D_s}z_0} - 1}, \tag{29}$$

where c_i is the concentration value on the melt side of the interface and T_i is the interfacial temperature. To determine the three constants T_i, c_i and z_0, we use the boundary conditions (20), (22) and (23) which in this case simplifies to

$$T_i = -m\, c_i, \tag{30}$$

$$\frac{1 - T_i}{e^{-\frac{1}{\kappa}(z_2-z_0)} - 1} = \frac{T_1 - T_i}{e^{\frac{1}{\kappa_s}z_0} - 1} + S_t, \tag{31}$$

$$c_i - \frac{c_2 - c_i}{e^{-\frac{1}{D}(z_2-z_0)} - 1} = k\, c_i - \frac{c_2 - k\, c_i}{e^{\frac{1}{D_s}z_0} - 1}, \tag{32}$$

In this case, the pressure $p = p^0(z)$ is hydrostatic and satisfies

$$\frac{dp^0}{dz} = \alpha\, g\, T^0 + \beta\, g\, (c^0 - c_2). \tag{33}$$

Note that all other equations and boundary conditions are trivially satisfied by the solutions (26)-(29) and (33) provided they satisfy (30)-(32).

An important limiting case (valid in many experiments) is that $\kappa/z_2 >> 1$, $\kappa_s/z_2 >> 1$. This simplifies expression for T^0 and T_s^0 as

$$T^0 \sim -mc_i + \frac{(z - z_0)}{z_2 - z_0}(1 + mc_i), \tag{34}$$

$$T_s^0 \sim -mc_i - \frac{(z - z_0)}{z_0}(T_1 + mc_i), \tag{35}$$

each of which is a linear function of z. In addition, when $(z_2 - z_0) >> D$, $S_t << \kappa/z_2$, $S_t << \kappa_s/z_2$ and $D_s << z_0$, (conditions that appear to be valid in some experiments), the matching conditions imply that the interfacial concentration

$$c_i \sim \frac{1}{k} c_2, \tag{36}$$

$$z_0 \sim z_2 \left\{ 1 + \frac{\kappa(1 + \frac{m}{k} c_2)}{\kappa_s(-\frac{m}{k} c_2 - T_1)} \right\}^{-1}. \tag{37}$$

Notice that the quantity $\frac{1+\frac{m}{k}c_2}{-\frac{m}{k}c_2 - T_1}$ is the ratio of the temperature difference between the top and the interface and the temperature difference between the interface and the bottom. Clearly, by controlling the location of the insulation zone, z_0 can be made to lie between $z = z_I$ and $z = z_{II}$, as will be assumed here.

Until we get to a discussion of the concrete formulae (212) and (213) for interfacial shape and radial segregation in sections 6 and 7, the only simplification that will be used is that each of T^0 and T_s^0 is a linear linear functions of z as in (34) and (35), since κ/z_2 and κ_s/z_2 are assumed large. Otherwise, the analysis will proceed with the assumption that each of c^0, T^0, c_s^0 and T_s^0 are known from (26)-(32).

4 Perturbed Steady state for nonzero ϵ

Now consider a small nonzero ϵ. In this case, the dependent variables can no longer just depend on z. As is well known, the presence of a radial thermal gradient means that the quiescent state is no longer a steady state solution to the problem. We express solutions as a perturbation expansion in powers of ϵ :

$$T = T^0 + \epsilon T^1 + .., \tag{38}$$

$$c = c^0 + \epsilon c^1 + .., \tag{39}$$

$$u = \epsilon u^1 + .., \tag{40}$$

$$w = -1 + \epsilon w^1 + .., \tag{41}$$

$$p = p^0 + \epsilon p^1 + .., \tag{42}$$

$$T_s = T_s^0 + \epsilon T_s^1 + .., \tag{43}$$

$$c_s = c_s^0 + \epsilon c_s^1 + .., \tag{44}$$

$$f = z_0 + \epsilon f^1 + \ldots . \tag{45}$$

Substituting these into (1-4), (6) and (7), and equating the ϵ terms in the resulting equations,

$$-\frac{\partial T^1}{\partial z} + w^1 T^{0\prime} = \kappa \nabla^2 T^1, \tag{46}$$

$$-\frac{\partial c^1}{\partial z} + w^1 c^{0\prime} = D \nabla^2 c^1, \tag{47}$$

$$-\frac{\partial u^1}{\partial z} = -\frac{\partial p^1}{\partial r} + \nu \nabla^2 u^1 - \frac{\nu}{r^2} u^1, \tag{48}$$

$$-\frac{\partial w^1}{\partial z} = -\frac{\partial p^1}{\partial z} + (\alpha T^1 + \beta c^1)\, g + \nu \nabla^2 w^1, \tag{49}$$

$$\frac{1}{r}\frac{\partial}{\partial r}(r u^1) + \frac{\partial}{\partial z} w^1 = 0. \tag{50}$$

On the solid side, we have

$$-\frac{\partial T_s^1}{\partial z} = \kappa_s \nabla^2 T_s^1, \tag{51}$$

$$-\frac{\partial c_s^1}{\partial z} = D_s \nabla^2 c_s^1. \tag{52}$$

We note that in this coordinate system, the operator ∇^2 is given by

$$\nabla^2 = \frac{\partial^2}{\partial r^2} + \frac{1}{r}\frac{\partial}{\partial r} + \frac{\partial^2}{\partial z^2}.$$

The boundary conditions on $r = 1$ for $z_0 < z < z_2$ are

$$u^1 = 0, \tag{53}$$

$$\frac{\partial w^1}{\partial r} = 0, \tag{54}$$

$$\frac{\partial c^1}{\partial r} = 0, \tag{55}$$

$$\frac{\partial T^1}{\partial r} = 0 \quad \text{for } z_0 < z < z_{II}, \tag{56a}$$

$$\frac{\partial T^1}{\partial r} + q_1 T^0 = q_2 \quad \text{for } z_{II} < z < z_2. \tag{56b}$$

On $r = 1$ for $0 < z < z_0$, from (12)-(13), we have the boundary conditions

$$\frac{\partial c_s^1}{\partial r} = 0, \tag{57}$$

$$\frac{\partial T_s^1}{\partial r} = 0 \quad \text{for } z_0 > z > z_I, \tag{58a}$$

$$\frac{\partial T_s^1}{\partial r} = -q_{1s} T_s^0 + q_{2s} \quad \text{for } z_I > z > 0. \tag{58b}$$

The boundary conditions at the top $z = z_2$ are

$$T^1 = 0, \tag{59}$$

$$c^1 = 0, \tag{60}$$

$$u^1 = 0, \tag{61}$$

$$w^1 = 0, \tag{62}$$

and at the bottom, $z = 0$,

$$T_s^1 = 0, \tag{63}$$

$$c_s^1 = 0. \tag{64}$$

On the original interface $z = z_0$, (20) implies

$$T_s^1 + f^1 T_s^{0\prime} = T^1 + f^1 T^{0\prime} = -m c^{0\prime} f^1 - m c^1 + d_0 \left\{ f^{1\prime\prime} + \frac{1}{r} f^{1\prime} \right\}. \tag{65}$$

From (21)-(25), we get

$$c_s^1 + f^1 c_s^{0\prime} = k c^1 + k f^1 c^{0\prime}, \tag{66}$$

$$-\kappa T^{0\prime\prime} f^1 - \kappa \frac{\partial T^1}{\partial z} = -\kappa_s T_s^{0\prime\prime} f^1 - \kappa_s \frac{\partial T_s^1}{\partial z}, \tag{67}$$

$$-D c^{0\prime\prime} f^1 - D \frac{\partial c^1}{\partial z} + (k-1) \left[c^1 + c^{0\prime} f^1 \right] = -D_s c_s^{0\prime\prime} f^1 - D_s \frac{\partial c_s^1}{\partial z}, \tag{68}$$

$$w^1 = 0, \tag{69}$$

$$u^1 = 0, \tag{70}$$

respectively. We can eliminate pressure from (48) and (49). Also, from (50), it follows that $\vec{v}^1 = (u^1, w^1) = curl\ \vec{A}$ for some vector field $\vec{A}$ that can be chosen to be divergence free. For the axisymmetric flow under consideration $\vec{A}$ can be reduced to a scalar 'stream function' ψ so that the velocity components of $\vec{v}^1$ can be written as

$$u^1 = -\frac{\partial \psi}{\partial z}, \tag{71}$$

$$w^1 = \frac{1}{r} \frac{\partial (r\psi)}{\partial r}. \tag{72}$$

Then, from (47) and (48), we get

$$-\frac{\partial}{\partial z} \left(\mathcal{L} + \frac{\partial^2}{\partial z^2} \right) \psi = \nu \left(\mathcal{L} + \frac{\partial^2}{\partial z^2} \right)^2 \psi + g \left[\alpha \frac{\partial T^1}{\partial r} + \beta \frac{\partial c^1}{\partial r} \right], \tag{73}$$

where the differential operator $\mathcal{L}$ is defined such that

$$\mathcal{L}\, u \;=\; \frac{\partial}{\partial r}\left\{\frac{1}{r}\,\frac{\partial (r\, u)}{\partial r}\right\}. \tag{74}$$

On taking the partial derivative of each of equations (46) and (47) with respect to r, we obtain

$$-\frac{\partial}{\partial z}\,\frac{\partial T^1}{\partial r} \;+\; T^{0\prime}\,\mathcal{L}\,\psi \;=\; \kappa\left(\mathcal{L} \;+\; \frac{\partial^2}{\partial z^2}\right)\,\frac{\partial T^1}{\partial r}, \tag{75}$$

$$-\frac{\partial}{\partial z}\,\frac{\partial c^1}{\partial r} \;+\; c^{0\prime}\,\mathcal{L}\,\psi \;=\; D\left(\mathcal{L} \;+\; \frac{\partial^2}{\partial z^2}\right)\,\frac{\partial c^1}{\partial r}. \tag{76}$$

On taking partial derivative of (51) and (52) with respect to r, we get

$$-\frac{\partial}{\partial z}\,\frac{\partial T_s^1}{\partial r} \;=\; \kappa_s\left(\mathcal{L} \;+\; \frac{\partial^2}{\partial z^2}\right)\,\frac{\partial T_s^1}{\partial r}, \tag{77}$$

$$-\frac{\partial}{\partial z}\,\frac{\partial c_s^1}{\partial r} \;=\; D_s\left(\mathcal{L} \;+\; \frac{\partial^2}{\partial z^2}\right)\,\frac{\partial c_s^1}{\partial r}. \tag{78}$$

The boundary conditions (53) and (54) imply that without any loss of generality,

$$\psi\,(1,z) \;=\; 0, \tag{79}$$

$$\mathcal{L}\,\psi(1,z) \;=\; 0, \tag{80}$$

while the boundary conditions (61),(62), (69) and (70) imply that

$$\psi(r,z_2) = 0, \tag{81}$$

$$\frac{\partial \psi}{\partial z}\,(r,z_2) \;=\; 0, \tag{82}$$

$$\psi\,(r,z_0) \;=\; 0, \tag{83}$$

$$\frac{\partial \psi}{\partial z}\,(r,z_0) \;=\; 0. \tag{84}$$

Further on taking the tangential derivative (i.e. derivative with respect to r) of each of the equations (65)-(68), we obtain

$$\frac{\partial T_s^1}{\partial r} \;+\; f^{1\prime}\,T_s^{0\prime} \;=\; \frac{\partial T^1}{\partial r} \;+\; f^{1\prime}\,T^{0\prime}, \tag{85}$$

$$\frac{\partial T^1}{\partial r} \;+\; f^{1\prime}\,T^{0\prime} \;=\; -m\,c^{0\prime}\,f^{1\prime} \;-\; m\,\frac{\partial c^1}{\partial r} \;+\; d_0\,\mathcal{L}\,f^{1\prime}, \tag{86}$$

$$\frac{\partial c_s^1}{\partial r} \;+\; f^{1\prime}\,c_s^{0\prime} \;=\; k\,\frac{\partial c^1}{\partial r} \;+\; k\,f^{1\prime}\,c^{0\prime}, \tag{87}$$

$$-\kappa\, T^{0\prime\prime}\, f^{1\prime} \;-\; \kappa\, \frac{\partial}{\partial z}\, \frac{\partial T^1}{\partial r} \;=\; -\kappa_s\, T_s^{0\prime\prime}\, f^{1\prime} \;-\; \kappa_s\, \frac{\partial}{\partial z}\, \frac{\partial T_s^1}{\partial r}, \tag{88}$$

$$-D\, c^{0\prime\prime}\, f^{1\prime} \;-\; D\, \frac{\partial}{\partial z}\, \frac{\partial c^1}{\partial r} \;+\; (k-1)\, \left[\frac{\partial c^1}{\partial r} + c^{0\prime}\, f^{1\prime}\right] = -D_s\, c_s^{0\prime\prime}\, f^{1\prime} \;-\; D_s\, \frac{\partial}{\partial z}\, \frac{\partial c_s^1}{\partial r}. \tag{89}$$

In addition to the above boundary conditions, elementary considerations of smoothness of each of the variables T^1 , T_s^1 , c^1 , c_s^1 and $\vec{v}^1$ in the neighborhood of $r = 0$ together with consideration of axisymmetrical flow, leads us to conclude that as $r \to 0$,

$$\psi \;\sim\; t_1\,(z)\, r, \tag{90}$$

$$\frac{\partial T^1}{\partial r} \;\sim\; t_2(z)\, r, \tag{91}$$

$$\frac{\partial T_s^1}{\partial r} \;\sim\; t_3(z)\, r, \tag{92}$$

$$\frac{\partial c^1}{\partial r} \;\sim\; t_4(z)\, r, \tag{93}$$

$$\frac{\partial c_s^1}{\partial r} \;\sim\; t_5(z)\, r, \tag{94}$$

$$f^{1\prime} \;\sim\; \text{constant } r \tag{95}$$

for some functions t_1 through t_5 , their precise form being unimportant.

5 Series representation of solution

The problem (equations (73), (75)-(78)) in conjunction with (55)-(60), (63), (64), (79)-(89) and assumptions (90)-(95) completely determine each of the unknown functions $\frac{\partial}{\partial r}T^1$, $\frac{\partial}{\partial r}c^1$, $\frac{\partial}{\partial r}T_s^1$, $\frac{\partial}{\partial r}c_s^1$ and ψ as functions of r and z and $f^{1\prime}$ as a function of r.

We expand each of the variables

$$\frac{\partial T^1}{\partial r} \;=\; \sum_{n=1}^{\infty} \frac{2}{J_1'(\lambda_n)}\, a_n\,(z)\, J_1(\lambda_n\, r), \tag{96}$$

$$\frac{\partial c^1}{\partial r} \;=\; \frac{\alpha}{\beta} \sum_{n=1}^{\infty} \frac{2}{J_1'(\lambda_n)}\, b_n\,(z)\, J_1(\lambda_n\, r), \tag{97}$$

$$\psi \;=\; \frac{g\alpha}{\nu} \sum_{n=1}^{\infty} \frac{2}{J_1'(\lambda_n)}\, c_n\,(z)\, J_1(\lambda_n\, r), \tag{98}$$

$$\frac{\partial T_s^1}{\partial r} \;=\; \sum_{n=1}^{\infty} \frac{2}{J_1'(\lambda_n)}\, a_n\,(z)\, J_1(\lambda_n\, r), \tag{99}$$

$$\frac{\partial c_s^1}{\partial r} \;=\; \frac{\alpha}{\beta} \sum_{n=1}^{\infty} \frac{2}{J_1'(\lambda_n)}\, b_n\,(z)\, J_1(\lambda_n\, r), \tag{100}$$

$$f^{1'} = \sum_{n=1}^{\infty} \frac{2}{J_1'(\lambda_n)} \; d_n \; J_1(\lambda_n \, r), \tag{101}$$

where λ_n is the n^{th} positive zero of the Bessel function J_1 . Notice that this is a suitable representation since

$$\mathcal{L} \; J_1(\lambda_n \, r) \; = \; -\lambda_n^2 \; J_1 \; (\lambda_n \, r)$$

and the boundary conditions (55), (57), (79) and (80) are automatically satisfied by each mode. The representation of $\frac{\partial T^1}{\partial r}$ and $\frac{\partial T_s^1}{\partial r}$ in (96) and (99) may appear to contradict (56b) and (58b). This is not the case since the convergence of the series in (96) and (99) for $z \; > \; z_{II}$ and $z \; < \; z_I$ is only in the mean and not pointwise at $r = 1$. In this range of z, there is a slow $\frac{1}{n}$ decay of a_n and a_{sn} as $n \; \rightarrow \; \infty$, which implies that one cannot calculate the derivative of the series (96) and (99) term by term. Thus, it is not possible to plug the series expressions directly into the differential equations and obtain the correct equations for a_n and a_{sn}. Instead, we multiply each of (73), (75)-(78), (85)-(89) by $r \; J_1 \; (\lambda_n \, r)$ and integrate with respect to r from 0 to 1. On integrating by parts, and using (55)-(58), (79), (80), (90)-(95) and the following relations:

$$a_n \; (z) \; = \; \frac{1}{J_1'(\lambda_n)} \; \int_0^1 \; dr \; r \; J_1(\lambda_n \, r) \; \frac{\partial T^1}{\partial r} \; (r, z),$$

$$b_n \; (z) \; = \; \frac{\beta}{\alpha \; J_1'(\lambda_n)} \; \int_0^1 \; dr \; r \; J_1(\lambda_n \, r) \; \frac{\partial c^1}{\partial r} \; (r, z),$$

$$c_n \; (z) \; = \; \frac{\nu}{g \; \alpha \; J_1'(\lambda_n)} \; \int_0^1 \; dr \; r \; J_1(\lambda_n \, r) \; \psi(r, z),$$

$$a_{sn} \; (z) \; = \; \frac{1}{J_1'(\lambda_n)} \; \int_0^1 \; dr \; r \; J_1(\lambda_n \, r) \; \frac{\partial T_s^1}{\partial r} \; (r, z),$$

$$b_{sn} \; (z) \; = \; \frac{\beta}{\alpha \; J_1'(\lambda_n)} \; \int_0^1 \; dr \; r \; J_1(\lambda_n \, r) \; \frac{\partial c_s^1}{\partial r} \; (r, z),$$

$$d_n \; = \; \frac{1}{J_1'(\lambda_n)} \; \int_0^1 \; dr \; r \; J_1(\lambda_n \, r) \; f(r),$$

we obtain three ordinary differential equations for each n on the melt side and two ordinary differential equations on the solid side. These equations can be written as

$$\mathcal{L}_2 \; b_n \; = \; \lambda_n^2 \; R_c \; h(z) \; c_n \quad \text{for} \quad z_0 \; < \; z \; < \; z_2 \; , \tag{102}$$

$$\mathcal{L}_3 \; c_n \; = \; -a_n \; - \; b_n \quad \text{for} \quad z_0 \; < \; z \; < \; z_2 \; , \tag{103}$$

$$\mathcal{L}_{1_m} \; a_n \; = \; -\lambda_n^2 \; R_T \; c_n \; + \; \lambda_n \; [\; -q_1 \; T^0 \; + \; q_2 \;] \quad \text{for} \quad z_{\text{II}} \; < \; z \; < \; z_2, \tag{104a}$$

$$\mathcal{L}_{1_m} \; a_n \; = \; -\lambda_n^2 \; R_T \; c_n \quad \text{for} \quad z_0 \; < \; z \; < \; z_{\text{II}}, \tag{104b}$$

$$\mathcal{L}_{2_s}\, b_{sn} \;=\; 0, \quad \text{for } 0 \;<\; z \;<\; z_0\,, \tag{105}$$

$$\mathcal{L}_{1_s}\, a_{sn} \;=\; \lambda_n\,[\,-q_{1_s}\, T_s^0 \;+\; q_{2_s}\,] \;\text{ for }\; 0 \;<\; z \;<\; z_I \tag{106a}$$

$$\mathcal{L}_{1_s}\, a_{sn} \;=\; 0 \;\text{ for }\; z_I \;<\; z \;<\; z_0 \tag{106b}$$

where

$$h(z) = e^{-(z-z_0)/D}, \tag{107}$$

$$R_T \;=\; \frac{gT^{0\prime}\alpha}{\kappa\nu}, \tag{108}$$

$$R_c \;=\; \frac{g\beta}{D\nu}\left(\frac{c_i \;-\; c_2}{1 \;-\; e^{-(z_2-z_0)/D}}\right) \tag{109}$$

and the differential operators

$$\mathcal{L}_{1_m} \;=\; \frac{d^2}{dz^2} \;+\; \frac{1}{\kappa}\,\frac{d}{dz} \;-\; \lambda_n^2 \quad,\quad \mathcal{L}_{1_s} \;=\; \frac{d^2}{dz^2} \;+\; \frac{1}{\kappa_s}\,\frac{d}{dz} \;-\; \lambda_n^2, \tag{110}$$

$$\mathcal{L}_2 \;=\; D\frac{d^2}{dz^2} \;+\; \frac{d}{dz} \;-\; \lambda_n^2\, D, \tag{111}$$

$$\mathcal{L}_3 \;=\; \left(\frac{d^2}{dz^2} \;-\; \lambda_n^2\right)^2 \;+\; \frac{1}{\nu}\left(\frac{d^2}{dz^2} \;-\; \lambda_n^2\right)\,\frac{d}{dz}, \tag{112}$$

$$\mathcal{L}_{2_s} \;=\; D_s\frac{d^2}{dz^2} \;+\; \frac{d}{dz} \;-\; \lambda_n^2\, D_s. \tag{113}$$

Note that since $\kappa/z_2 \;>>\; 1$, (34) holds and therefore $T^{0\prime}$ is a constant. So the thermal Rayleigh number R_T defined in (108) is also a constant (Note the definition in terms of dimensional variables as well in Table 2).

From (59)-(60), (81) and (82), we find that at the cylinder top,

$$a_n(z_2) \;=\; 0, \tag{114}$$

$$b_n\,(z_2) \;=\; 0, \tag{115}$$

$$c_n\,(z_2) \;=\; 0, \tag{116}$$

$$c_n'\,(z_2) \;=\; 0. \tag{117}$$

The boundary conditions (63),(64) at the cylinder bottom imply

$$a_{sn}(0) \;=\; 0, \tag{118}$$

$$b_{sn}\,(0) \;=\; 0. \tag{119}$$

At $z \;=\; z_0$, we find from (85)-(8[illegible] that

$$a_{sn}(z_0) \;+\; d_n\, T_s^{0\prime}(z_0) \;=\; a_n(z_0) \;+\; d_n\, T^{0\prime}(z_0), \tag{120}$$

$$a_n(z_0) + d_n T^{0\prime}(z_0) = -m c^{0\prime}(z_0) d_n - m \frac{\alpha}{\beta} b_n(z_0) - d_0 \lambda_n^2 d_n, \tag{121}$$

$$b_{sn}(z_0) + d_n \frac{\beta}{\alpha} c_s^{0\prime}(z_0) = k b_n(z_0) + k d_n \frac{\beta}{\alpha} c^{0\prime}(z_0), \tag{122}$$

$$-\kappa a_n'(z_0) - \kappa d_n T^{0\prime\prime}(z_0) = -\kappa_s a_{sn}'(z_0) - \kappa_s d_n T_s^{0\prime\prime}(z_0), \tag{123}$$

$$-Db_n'(z_0) - Dd_n\frac{\beta}{\alpha}c^{0\prime\prime}(z_0)+(k-1)[b_n(z_0)+c^{0\prime}(z_0)\frac{\beta}{\alpha}d_n] = -D_s b_{sn}'(z_0)-D_s d_n\frac{\beta}{\alpha}c_s^{0\prime\prime}(z_0). \tag{124}$$

From (83) and (84), it follows that

$$c_n(z_0) = 0, \tag{125}$$

$$c_n'(z_0) = 0. \tag{126}$$

Before proceeding further, for purposes of reducing algebra, we simplify the equations further by assuming that

(a) κ, κ/z_2, κ_s and $\kappa_s/z_2 >> 1$

(b) $d_0 = 0$

With the assumption (a) as above, we replace equations (104a,b) and (106a,b) by simpler equations

$$\mathcal{L}_1 a_n = -\lambda_n^2 R_T c_n + \lambda_n [-q_1 T^0 + q_2] \quad \text{for } z_{II} < z < z_2, \tag{127a}$$

$$\mathcal{L}_1 a_n = -\lambda_n^2 R_T c_n \quad \text{for } z_0 < z < z_{II}, \tag{127b}$$

$$\mathcal{L}_1 a_{sn} = \lambda_n [-q_{1_s} T_s^0 + q_{2_s}] \quad \text{for } 0 < z < z_I, \tag{128a}$$

$$\mathcal{L}_1 a_{sn} = 0 \quad \text{for } z_I < z < z_0, \tag{128b}$$

where

$$\mathcal{L}_1 = \frac{d^2}{dz^2} - \lambda_n^2. \tag{129}$$

The interfacial matching conditions (120)-(124) couple the concentration and temperature fields in the solid side to the melt variables. Using (105), (118), (119) and (128), expression for a_{sn} and b_{sn} can be obtained in terms of two arbitrary constants. By eliminating these arbitrary constants between $a_{sn}(z_0)$, $a_{sn}'(z_0)$ and $b_{sn}(z_0)$, $b_{sn}'(z_0)$, the matching conditions (120)-(124) can be written as two effective boundary conditions at $z = z_0$ on the melt variables. As shown in Appendix A, these boundary conditions are

$$\frac{1}{\lambda_n}a_n'(z_0) + \beta_1 a_n(z_0) + \beta_2 b_n(z_0) = \frac{\beta_3}{\lambda_n}e^{-\lambda_n(z_0-z_I)}, \tag{130}$$

$$b_n'(z_0) + m_1 b_n(z_0) + m_2 a_n(z_0) = 0, \tag{131}$$

where the effective interfacial parameters β_1, β_2, m_1, m_2 and β_3 are defined as:

$$\beta_1 = -\frac{\kappa_s(T_s^{0\prime} + mc^{0\prime}(z_0))(1 + e^{-2\lambda_n z_0})}{\kappa(mc^{0\prime}(z_0) + T^{0\prime})(1 - e^{-2\lambda_n z_0})}, \tag{132}$$

$$\beta_2 = -\frac{\kappa_s m\alpha(T_s^{0\prime} - T^{0\prime})(1 + e^{-2\lambda_n z_0})}{\kappa\beta(mc^{0\prime}(z_0) + T^{0\prime})(1 - e^{-2\lambda_n z_0})} \tag{133}$$

$$\beta_3 = -\frac{\kappa_s \left\{(q_{1_s}T_s^0(z_I) - q_{2_s})(1 + e^{-2\lambda_n z_I}) - 2(q_{1_s}T_1 - q_{2_s})e^{-\lambda_n z_I} - \frac{q_{1_s}}{\lambda_n}T_s^{0\prime}(1 + e^{-2\lambda_n z_I})\right\}}{\kappa\left[1 - e^{-2\lambda_n z_0}\right]}, \tag{134}$$

$$m_1 = \beta_4 + \hat{X}_2\beta_5, \tag{135}$$

$$m_2 = \beta_6 + \hat{X}_2\beta_7. \tag{136}$$

In the above expressions,

$$\beta_4 = -\frac{k-1}{D} + \frac{m\left(\frac{D_s}{D}c_s^{0\prime\prime}(z_0) + \frac{(k-1)}{D}c^{0\prime}(z_0) - c^{0\prime\prime}(z_0)\right)}{(T^{0\prime} + mc^{0\prime}(z_0))}, \tag{137}$$

$$\beta_5 = -\frac{D_s\left(mc_s^{0\prime}(z_0) + kT^{0\prime}\right)}{D(mc^{0\prime}(z_0) + T^{0\prime})}, \tag{138}$$

$$\beta_6 = \frac{\beta\left(\frac{D_s}{D}c_s^{0\prime\prime}(z_0) + \frac{(k-1)}{D}c^{0\prime}(z_0) - c^{0\prime\prime}(z_0)\right)}{\alpha\left(T^{0\prime} + mc^{0\prime}(z_0)\right)}, \tag{139}$$

$$\beta_7 = \frac{D_s\beta\left(kc^{0\prime}(z_0) - c_s^{0\prime}(z_0)\right)}{D\alpha(mc^{0\prime}(z_0) + T^{0\prime})}, \tag{140}$$

$$\hat{X}_2 = \frac{p_3 - p_4 e^{z_0(p_4 - p_3)}}{1 - e^{z_0(p_4 - p_3)}}, \tag{141}$$

$$p_{3,4} = -\frac{1}{2D_s} \pm \sqrt{\frac{1}{4D_s^2} + \lambda_n^2}, \tag{142}$$

6 Determination of solution in the melt

From (102), (103) and (127), we get an eight order linear differential equation for c_n :

$$\left[\mathcal{L}_1\mathcal{L}_2\mathcal{L}_3 + \lambda_n^2 R_c\mathcal{L}_1 h(z) - \lambda_n^2 R_T\mathcal{L}_2\right] c_n = \mathcal{L}_2\left[-\lambda_n[-q_1T^0 + q_2]\right] \text{ for } z_{II} < z < z_2, \tag{143a}$$

$$\left[\mathcal{L}_1\mathcal{L}_2\mathcal{L}_3 + \lambda_n^2 R_c\mathcal{L}_1 h(z) - \lambda_n^2 R_T\mathcal{L}_2\right] c_n = 0 \text{ for } z_0 < z < z_{II}. \tag{143b}$$

Alternatively, instead of one equation for c_n, we can write the following equations for c_n and a_n

$$\left[\mathcal{L}_3\mathcal{L}_2 - D\lambda_n^2 R_T + \lambda_n^2 R_c h(z)\right] c_n + a_n' = -D\lambda_n[-q_1T^\theta + q_2] \text{ for } z_{II} < z < z_2, \tag{144a}$$

$$\left[\mathcal{L}_3\mathcal{L}_2 - D\lambda_n^2 R_T + \lambda_n^2 R_c h(z)\right] c_n + a_n' = 0 \quad \text{for } z_0 < z < z_{II}, \tag{144b}$$

$$\mathcal{L}_1 a_n = -\lambda_n^2 R_T c_n + \lambda_n[-q_1T^0 + q_2] \text{ for } z_{II} < z < z_2, \tag{145a}$$

$$\mathcal{L}_1 a_n = -\lambda_n^2 R_T c_n \quad \text{for} \quad z_0 < z < z_{II} \ . \tag{145b}$$

The boundary conditions are (125), (126), (130) and (131) at $z = z_0$ and (114)-(117) at $z = z_2$. In addition, we require that a_n and its first derivative, b_n and its first derivative and c_n and all its first three derivatives are all continuous at $z = z_{II}$. From (103), this is equivalent to requiring that a_n and its first derivative, c_n and its first five derivatives are all continuous at $z = z_{II}$. These are enforced on a suitable representation of the general solution, as will be discussed shortly.

Since (143a) is an eighth order non homogeneous linear equation, we can express the general solution for $z_{II} < z < z_2$ in the form

$$c_n = c_{n_p}(z) + \sum_{j=1}^{2} \gamma^{-7} C_j F_j^c(z) + \sum_{j=3}^{8} \gamma^{-5} C_j F_j^c(z), \tag{146}$$

where $c_{np}(z)$ is a particular solution to (143a), F_j^c are eight independent solutions to the homogeneous equation (143b) and

$$\gamma = \lambda_n^{1/3} R_T^{1/6}. \tag{147}$$

Factors containing powers of γ in (146) can be absorbed as part of arbitrary constant C_j by suitable redefinition. We choose not to do so for we want to explicitly show the R_T scaling of the eventual answer. With our choice of C_j, it will turn out $C_j = O(1)$ as $R_T \to \infty$. Questions of determination of functions F_j^c and c_{np} will be set aside for the moment. Once c_n is obtained, expression for a_n and b_n be found, at least in principle from (144), (145) and (103). We write these symbolically in the form

$$a_n = a_{n_p}(z) + \sum_{j=1}^{8} \gamma^{-1} C_j F_j^a(z) \ , \tag{148}$$

$$b_n = b_{n_p} + \sum_{j=1}^{2} \gamma^{-1} C_j F_j^b(z) + \frac{\lambda_n^2 R_c}{\gamma^6} \sum_{j=3}^{8} C_j F_j^b(z) \ , \tag{149}$$

where F_j^a, F_j^b are related to F_j^c; while particular solutions a_{n_p} and b_{n_p} are determined in terms of c_{n_p}.

For $z_0 < z < z_{II}$, i.e. in the insulated zone, we write

$$c_n = \sum_{j=1}^{2} \gamma^{-7} \tilde{C}_j F_j^c + \sum_{j=3}^{8} \gamma^{-5} \tilde{C}_j F_j^c \tag{150}$$

$$a_n = \sum_{j=1}^{8} \gamma^{-1} \tilde{C}_j F_j^a \tag{151}$$

$$b_n = \sum_{j=1}^{2} \gamma^{-1} \tilde{C}_j F_j^b + \frac{\lambda_n^2 R_c}{\gamma^6} \sum_{j=3}^{8} \tilde{C}_j F_j^b \tag{152}$$

In appendix B, we derive asymptotic representation for each of F_j^c, F_j^a, F_j^b, c_{n_p}, a_{n_p} and b_{n_p} for large R_T that is uniformly valid for all λ_n, provided $|R_c| << R_T$. We also derive simpler expressions for the special case $R_T >> 1$ with $\gamma^5 >> \lambda_n^2 R_c$ and this latter expressions will be quoted here as these are the only ones needed in obtaining concrete results for $|R_c| << R_T^{5/6}$.

In the special case, $\lambda_n^2 |R_c| << \gamma^5$, the leading order asymptotic behavior is given by:

$$c_{np} \sim \frac{\lambda_n[-q_1 T^0 + q_2]}{[\lambda_n^2 R_T + \lambda_n^6]} - \frac{\lambda_n^5 q_1 T^{0'}}{\nu[\lambda_n^2 R_T + \lambda_n^6]^2}, \tag{153}$$

$$F_1^c \sim \frac{p_1}{D} e^{p_1(z-z_0)} \quad F_2^c \sim \frac{p_2}{D} e^{p_2(z-z_2)}, \tag{154}$$

$$F_j^c \sim e^{\gamma_j(z-z_0)} \text{ for } j = 3,4,5 \ , \tag{155}$$

$$F_j^c \sim e^{\gamma_j(z-z_2)} \text{ for } j = 6,7,8 \ , \tag{156}$$

where p_1 and p_2 are given by

$$p_{1,2} = -\frac{1}{2D} \mp \sqrt{\frac{1}{4D^2} + \lambda_n^2}. \tag{157}$$

Also, γ_j for j =3 to 8 are the six independent roots of

$$L_1[\gamma_j] L_3[\gamma_j] - \lambda_n^2 R_T = 0, \tag{158}$$

where

$$L_1[y] = y^2 - \lambda_n^2,$$

$$L_3[y] = (y^2 - \lambda_n^2)^2 + \frac{y}{\nu}(y^2 - \lambda_n^2).$$

The roots of (158) are labelled such that for $R_T >> \lambda_n^4$,

$$\gamma_j \sim \gamma \omega_j \tag{159}$$

where

$$\omega_3 = -e^{i\pi/3} = -\omega_8 \tag{160}$$

$$\omega_4 = -1 = -\omega_7 \tag{161}$$

$$\omega_5 = -e^{-i\pi/3} = -\omega_6 \tag{162}$$

a_{np} is general is a complicated expression, given in the appendix. We will not need the general expression in what follows except to not that in the special case when $\lambda_n^4 << R_T$, the general expression simplifies such that

$$a_{np} \sim -\frac{\lambda_n^5[-q_1T^0+q_2]}{\lambda_n^2R_T+\lambda_n^6} - \frac{\lambda_n^5 q_1 T^{0'} R_T}{\nu[\lambda_n^2R_T+\lambda_n^6]^2} - \frac{\lambda_n^2 R_c h(z)}{L_2[-D^{-1}]}\left[c_{np} + \frac{c'_{np}}{L_2[-D^{-1}]}\right], \tag{163}$$

where

$$L_2[y] = D(y^2-\lambda_n^2)+y.$$

For $\gamma^5 >> \lambda_n^2|R_c|$ (λ_n unrestricted otherwise),

$$F_1^a \sim e^{p_1(z-z_0)} \quad F_2^a \sim e^{p_2(z-z_2)}, \tag{164}$$

$$F_j^a \sim -\frac{\gamma^2}{\gamma_j^2-\lambda_n^2}\, e^{\gamma_j(z-z_0)} \text{ for } j=3,4,5\ , \tag{165}$$

$$F_j^a \sim -\frac{\gamma^2}{\gamma_j^2-\lambda_n^2}\, e^{\gamma_j(z-z_2)} \text{ for } j=6,7,8\ . \tag{166}$$

The asymptotic form of b_{np} is simply obtained by using

$$b_{np} = -a_{np} - \mathcal{L}_3[c_{np}] \tag{167}$$

For $\gamma^5 >> \lambda_n^2|R_c|$, The independent homogeneous solutions for b_n have the asymptotic behavior

$$F_1^b \sim -e^{p_1(z-z_0)}\ , \quad F_2^b \sim -e^{p_2(z-z_2)}\ , \tag{168}$$

$$F_j^b \sim -e^{\gamma_j(z-z_0)}\frac{\gamma D L_1[\hat{\gamma}_j]}{\hat{\gamma}_j L_2[\hat{\gamma}_j]}h(z) + .. \text{ for } j=3,4,5\ , \tag{169}$$

$$F_j^b \sim -e^{\gamma_j(z-z_2)}\frac{\gamma D L_1[\hat{\gamma}_j]}{\hat{\gamma}_j L_2[\hat{\gamma}_j]}h(z) + .. \text{ for } j=6,7,8\ , \tag{170}$$

where

$$\hat{\gamma}_j = \gamma_j - \frac{1}{D}$$

These asymptotic results for a special case will be used later in obtaining concrete expressions for quantities of interest. It is to be noted that the asymptotic expressions (155), (156), (165), (166), (169), (170) become invalid when $|\lambda_n^2 R_c|$ is the same order as γ^5 or larger. This can occur even for $R_c << R_T^{5/6}$ provided λ_n is large enough. In Appendix B, section 2, we derive more general expressions for the solution of the homogeneous equation will be uniformly valid for all λ_n provided $R_T << R_c$. The expressions (155), (156), (165), (166), (169) and (170) will have to be replaced by these expressions. The remaining asymptotic relations (153), (154), (163), (164), (167) and (168), however, remain valid in this range of parameters.

Despite differing asymptotics in different regimes, at this stage we prefer to think of relations (146)-(152) as exact. The only aspects of the asymptotic results of Appendix B in differing regimes that will be used in this part of our analysis is that in all cases,
(i) Each of F_j^c, F_j^b and F_j^a have a common exponential part $e^{W_j(z)}$ multiplied by an algebraic dependent term that depend on superscript a, b or c. For instance, when $\lambda_n^2|R_c| << \gamma^5$,

$$W_1 = p_1(z-z_0),\ W_2 = p_2(z-z_2),\ W_j = \gamma_j(z-z_0) \text{ for } j = 3,4,5\ \ W_j = \gamma_j(z-z_2) \text{ for } j = 6,7,8 \tag{171}$$

(ii) The variation in z of e^{W_j} for $j = 3,4..8$ is much larger than the variation of the algebraic prefactors when $R_T >> 1$, while for $\lambda_n >> 1$, the variation of the exponential part e^{W_j} for $j = 1,2$ dominate the variation of the prefactors.
(iii) For $j = 1,3,4,5$, $Re\ W_j' > 0$, while for $j = 2,6,7,8$, $Re\ W_j' < 0$.
(iv) The choice of the constants C_j and $\tilde{C}_j$ and the prefactors is such that $W_j(z_0) = 0$ for $j = 1,3,4,5$, while $W_j(z_2) = 0$ for $j = 2,6,7,8$.

As a consequence of the above properties, it is clear that for large R_T, we have each of $F_j^c(z_0)$, $F_j^a(z_0)$ and $F_j^b(z_0)$ will be exponentially small in R_T for $j = 6,7,8$, while $F_j^c(z_2)$, $F_j^a(z_2)$ and $F_j^b(z_2)$ are exponentially small in R_T for $j = 3,4,5$. Again for $\lambda_n >> 1$, each of $F_2^a(z_0)$, $F_2^b(z_0)$, $F_2^c(z_0)$, $F_1^a(z_2)$, $F_1^b(z_2)$ and $F_1^c(z_2)$ is exponentially small in λ_n. These facts will be needed later in simplifying matrix equations.

The continuity of a_n and its first derivative, c_n and its first five derivatives can be written as the following matrix relation

$$GX = R, \tag{172}$$

where G is a 8×8 matrix, X and R are column vectors with 8 entries. These are defined such that for $j = 1,2$,

$$X_j = \gamma^{-1}(\tilde{C}_j - C_j)e^{W_j(z_{II})}, \tag{173}$$

$$R_j = \frac{d^{(j-1)}}{dz^{(j-1)}}_{z=z_{II}} a_{n_p}, \tag{174}$$

$$G_{k,j} = e^{-W_j(z_{II})}\frac{d^{(k-1)}}{dz^{(k-1)}}|_{z=z_{II}}\ F_j^a \ \text{ for k} = 1,2\ , \tag{175}$$

and

$$G_{k,j} = \gamma^{-(k-2)}\ e^{-W_j(z_{II})}\ \frac{d^{(k-3)}}{dz^{(k-3)}}|_{z=z_{II}}\ F_j^c \ \text{ for k} = 3,4,..8. \tag{176}$$

For $j = 3$,...8,

$$X_j = (\tilde{C}_j - C_j)e^{W_j(z_{II})}, \tag{177}$$

$$R_j = \gamma^{8-j}\frac{d^{(j-1)}}{dz^{(j-1)}}|_{z=z_{II}}\ c_{n_p}, \tag{178}$$

$$G_{k,j} = \gamma^{-1}e^{-W_j(z_{II})}\frac{d^{(k-1)}}{dz^{(k-1)}}|_{z=z_{II}}\ F_j^a \ \text{ for k} = 1,2\ , \tag{179}$$

and

$$G_{k,j} = \gamma^{-(k-3)} e^{-W_j(z_{II})} \frac{d^{(k-3)}}{dz^{(k-3)}}_{z=z_{II}} F_j^c \quad \text{for} \quad \mathrm{k} = 3,4,..8. \tag{180}$$

Note that in arriving at (172)-(180), we had to scale the original continuity equations with appropriate powers of γ. Further, we scaled the unknown X with $e^{W_j(z_{II})}$. These steps are necessary to ensure that the limiting G as $R_T \rightarrow \infty$ (i.e. $\gamma \rightarrow \infty$) is non-singular and free of transcendental terms in R_T.

Denoting

$$H = G^{-1}, \tag{181}$$

it is clear that we can then write for $j = 1,2$,

$$\tilde{C}_j = C_j + \gamma e^{-W_j(z_{II})} \sum_{k=1}^{8} H_{j,k} R_k, \tag{182}$$

while for $j = 3,..8$, we have

$$\tilde{C}_j = C_j + e^{-W_j(z_{II})} \sum_{k=1}^{8} H_{j,k} R_k. \tag{183}$$

We satisfy (125), (126), (130) and (131) at $z = z_0$ and (114)-(117) at $z = z_2$, which on using (182) and (183), is equivalent to the matrix relation

$$MZ = S, \tag{184}$$

where M is a 8×8 matrix, while Z and S are each column vectors with eight entries. These are defined such that

$$Z = (\tilde{C}_1, C_2, \tilde{C}_3, \tilde{C}_4, \tilde{C}_5, C_6, C_7, C_8)^T, \tag{185}$$

$$\begin{aligned} S = \; & (0,0,\lambda_n^{-1}\beta_3 e^{-\lambda_n(z_0-z_I)}, 0, 0, -\gamma a_{n_p}(z_2), -\gamma^5 c_{n_p}(z_2), -\gamma^4 c'_{n_p}(z_2), -\gamma b'_{n_p}(z_2))^T \\ & + (P_1, P_2, P_3, P_4, P_5, P_6, P_7, P_8)^T \quad , \end{aligned} \tag{186}$$

where for $1 \leq l \leq 4$,

$$P_l = -\gamma M_{l,2} e^{-W_2(z_{II})} \sum_{j=1}^{8} H_{2,j} R_j - \sum_{k=6}^{8} M_{l,k} e^{-W_k(z_{II})} \sum_{j=1}^{8} H_{k,j} R_j \tag{187}$$

and for $5 \leq l \leq 8$,

$$P_l = \gamma M_{l,1} e^{-W_1(z_{II})} \sum_{j=1}^{8} H_{1,j} R_j + \sum_{k=3}^{5} M_{l,k} e^{-W_k(z_{II})} \sum_{j=1}^{8} H_{k,j} R_j. \tag{188}$$

The elements of the matrix M can be written as

$$M_{1,j} = \gamma^{-2} F_j^c(z_0), \quad \text{for j} = 1,2 \;\; \text{and} \;\; \mathrm{M_{1j}} = \mathrm{F_j^c}(z_0) \quad \text{for j} = 3,4..,8, \tag{189}$$

$$M_{2,j} = \gamma^{-3} F_j^{c'}(z_0), \quad \text{for j} = 1,2 \text{ and } \mathrm{M_{2,j}} = \gamma^{-1}\mathrm{F_j^{c'}}(\mathrm{z_0}) \quad \text{for j} = 3,4..,8 \tag{190}$$

$$M_{3,j} = \gamma^{-1}\left[\lambda_n^{-1} F_j^{a'} + \beta_1 F_j^a + \beta_2 F_j^b\right]_{z_0} \quad \text{for j} = 1,2, \tag{191}$$

$$M_{3,j} = \left[\gamma^{-1}\lambda_n^{-1} F_j^{a'} + \gamma^{-1}\beta_1 F_j^a + \beta_2 \lambda_n^2 R_c \gamma^{-6} F_j^b\right]_{z_0} \quad \text{for j} = 3,4..,8\ , \tag{192}$$

$$M_{4,j} = \left[\lambda_n^{-1} F_j^{b'} + m_1 F_j^b + m_2 F_j^b\right]_{z_0} \quad \text{for j} = 1,2, \tag{193}$$

$$M_{4,j} = \frac{\lambda_n^2 R_c}{\gamma^5}\left[F_j^{b'} + m_1 F_j^b\right]_{z_0} + m_2 F_j^a(z_0) \quad \text{for j} = 3,4..,8\ , \tag{194}$$

$$M_{5,j} = F_j^a(z_2) \quad \text{for j} = 1,2,..8, \tag{195}$$

$$M_{6,j} = \gamma^{-2} F_j^c(z_2), \quad \text{for j} = 1,2 \text{ and } \mathrm{M_{6,j}} = \mathrm{F_j^c}(\mathrm{z_2}) \quad \text{for j} = 3,4..,8, \tag{196}$$

$$M_{7,j} = \gamma^{-3} F_j^{c'}(z_2), \quad \text{for j} = 1,2 \text{ and } \mathrm{M_{7,j}} = \gamma^{-1}\mathrm{F_j^{c'}}(\mathrm{z_2}) \quad \text{for j} = 3,4..,8, \tag{197}$$

$$M_{8,j} = F_j^b(z_2), \quad \text{for j} = 1,2 \text{ and } \mathrm{M_{8,j}} = \lambda_n^2 \mathrm{R_c}\gamma^{-5}\mathrm{F_j^b}(\mathrm{z_2}) \quad \text{for j} = 3,4..,8. \tag{198}$$

Note that in arriving at the specific form of matrix M, which is nonsingular in the asymptotic limit of $R_T \rightarrow \infty$, we needed to multiply each of the original boundary conditions by appropriate scale factors involving γ. Once solution $Z = M^{-1}S$ is found to (184), the quantities $a_n(z_0)$ and $b_n(z_0)$ can be written in terms of Z as:

$$a_n(z_0) = \gamma^{-1}\left\{F_1^a(z_0)Z_1 + F_2^a(z_0)\left(Z_2 + \gamma e^{-W_2(z_{11})}\sum_{k=1}^{8} H_{2,k}R_k\right)\right\}$$

$$+\gamma^{-1}\sum_{j=3}^{5} F_j^a(z_0)Z_j + \gamma^{-1}\sum_{j=6}^{8} F_j^a(z_0)\left(Z_j + e^{-W_j(z_{11})}\sum_{k=1}^{8} H_{j,k}R_k\right), \tag{199}$$

$$b_n(z_0) = \gamma^{-1}\left\{F_1^b(z_0)Z_1 + F_2^b(z_0)\left(Z_2 + \gamma e^{-W_2(z_{11})}\sum_{k=1}^{8} H_{2,k}R_k\right)\right\}$$

$$+\frac{\lambda_n^2 R_c}{\gamma^6}\sum_{j=3}^{5} F_j^b(z_0)Z_j + \frac{\lambda_n^2 R_c}{\gamma^6}\sum_{j=6}^{8} F_j^b(z_0)\left(Z_j + e^{-W_j(z_{11})}\sum_{k=1}^{8} H_{j,k}R_k\right). \tag{200}$$

In terms of $a_n(z_0)$ and $b_n(z_0)$, as shown in Appendix A, the interfacial deformation coefficient

$$d_n = -\frac{a_n(z_0) + \frac{m\alpha}{\beta}b_n(z_0)}{T^{0'} + mc^{0'}(z_0)}, \tag{201}$$

and the radial segregation coefficient

$$b_{sn}(z_0) = d_n\frac{\beta}{\alpha}\left(kc^{0'}(z_0) - c_s^{0'}(z_0)\right) + kb_n(z_0). \tag{202}$$

Recall that the function e^{W_j} reflects the common exponential part of the growth for the functions F_j^a, F_j^b and F_j^c. As discussed earlier, and shown explicitly in appendix B, for $R_T >> |R_c|$, with $R_T >> 1$, e^{W_j} for $j = 3,4,5$ decreases exponentially at a large rate with

increasing z from a value of 1 at $z = z_0$. This is uniformly true for all λ_n. The decrease is at least like $O(e^{-\frac{1}{2}\gamma(z-z_0)})$ Further, e^{W_j} for $j = 6,7,8$ decreases exponentially with decreasing z from a value of 1 at $z = z_2$ at a rate that is at least $O(e^{-\frac{1}{2}\gamma(z_2-z)})$. Thus, the elements $M_{k,j}$ for $1 \leq k \leq 4, 6 \leq j \leq 8$ and for $5 \leq k \leq 8, 3 \leq j \leq 5$ are $O(e^{-\frac{1}{2}\gamma(z_2-z_0)})$, which is exponentially small in R_T. Further, if $\lambda_n >> 1$, it is clear from (157) that $p_1 \sim -\lambda_n$ and $p_2 \sim \lambda_n$ and so $M_{k,2}$ for $1 \leq k \leq 4$ and $M_{k,1}$ for $5 \leq k \leq 8$ are each $O(e^{-\lambda_n(z_2-z_0)})$, which is transcendentally small in λ_n. Thus, if λ_n or $z_2 - z_0$ is of the order of some positive power of R_T, these terms will also be transcendentally small in R_T. Further, using the growing and decreasing properties of e^{W_j}, it is easy to see that the the elements P_l defined in (187), (188) satisfy

$$P_l = O\left(e^{-\lambda_n(z_{II}-z_0)}, e^{-\frac{1}{2}\gamma(z_{II}-z_0)}, e^{-\frac{\gamma}{2}(z_2-z_{II})}, e^{-\lambda_n(z_2-z_{II})}\right). \tag{203}$$

Further, the term $\lambda_n^{-1}\beta_3 e^{-\lambda_n(z_0-z_I)}$ appearing in the third element of S in (186) is transcendentally small in λ_n for large λ_n. Noticing the special structure of the reduced matrix M, obtained by ignoring transcendentally small elements in the limit of large λ_n and R_T, it is clear that the solution Z to (184) has components

$$Z_j = O\left(e^{-\lambda_n(z_{II}-z_0)}, e^{-\frac{1}{2}\gamma(z_{II}-z_0)}, e^{-\lambda_n(z_0-z_I)}\right) \quad \text{for} \quad j = 1,3,4,5, \tag{204}$$

Further, $Z_2 = O(1)$ and each Z_j for $j = 6,7,8$ are at best $O(1)$ and so

$$e^{W_2(z_0)}\left(Z_2 + e^{-W_2(z_{II})}\gamma\sum_{l=1}^{8} H_{2,l}R_l\right) = O\left(e^{-\lambda_n(z_{II}-z_0)}\right), \tag{205}$$

$$e^{W_j(z_0)}\left(Z_j + e^{-W_j(z_{II})}\sum_{l=1}^{8} H_{j,l}R_l\right) = O\left(e^{-\frac{\gamma}{2}(z_{II}-z_0)}\right) \quad \text{for } j = 6,7,8. \tag{206}$$

Thus, from (199)-(206), it follows that the effect of the insulation zone is to exponentially quench the small scale components of the radial segregation and interfacial deformation, which correspond to $b_{sn}(z_0)$ and d_n for large λ_n. Most of the contribution in the summations (96)-(101) therefore comes from terms where $\lambda_n = O(1)$.

In that case, the matrices G and M simplify further in the asymptotic limit $R_T >> 1$. As shown in appendix C, (184) can be solved in closed form in this asymptotic limit resulting in $(Z_6, Z_7, Z_8) = o(1)$,

$$(Z_3, Z_4, Z_5) \sim \left(-\frac{1}{2} + i\frac{\sqrt{3}}{6}, 1, -\frac{1}{2} - i\frac{\sqrt{3}}{6}\right)\beta_3 e^{-\lambda_n(z_0-z_I)} \tag{207}$$

$$(Z_1, Z_2) \sim -\frac{2m_2\beta_3 e^{-\lambda_n(z_0-z_I)}}{(p_1 + m_1 - m_2) - e^{(p_1-p_2)(z_2-z_0)}(p_2 + m_1 - m_2))}\left(1, -e^{p_1(z_2-z_0)}\right), \tag{208}$$

where the effective parameters β_3, m_1 and m_2 are as defined in (134)-(136). From (199) and (200) and the above asymptotic results,

$$a_n(z_0) \sim -2\gamma^{-1}\beta_3 e^{-\lambda_n(z_0-z_I)}\left[1+\frac{m_2[1-e^{(p_1-p_2)(z_2-z_0)}]}{[p_1+m_1-m_2-e^{(p_1-p_2)(z_2-z_0)}(p_2+m_1-m_2)]}\right] \quad (209)$$

$$b_n(z_0) \sim 2\gamma^{-1}\beta_3 e^{-\lambda_n(z_0-z_I)}\frac{m_2[1-e^{(p_1-p_2)(z_2-z_0)}]}{[p_1+m_1-m_2-e^{(p_1-p_2)(z_2-z_0)}(p_2+m_1-m_2)]} \quad (210)$$

From (201), we find

$$d_n \sim 2\beta_3\gamma^{-1}\frac{e^{-\lambda_n(z_0-z_I)}}{(T^{0\prime}+mc^{0\prime}(z_0))}\left[1+\frac{m_2(1-m\frac{\alpha}{\beta})\left\{1-e^{(p_1-p_2)(z_2-z_0)}\right\}}{(p_1+m_1-m_2-(p_2+m_1-m_2)e^{(p_1-p_2)(z_2-z_0)})}\right] \quad (211)$$

From (202), (210) and (211), we can obtain asymptotic expression for $b_{sn}(z_0)$ as well. From (45), (101) and recalling that $J_1'(\lambda_n) = J_0(\lambda_n)$, we get interfacial slope

$$f'(r) \sim \sum_{n=1}^{\infty}\frac{J_1(\lambda_n r)}{\lambda_n^{1/3}J_0(\lambda_n)}\frac{4\epsilon\beta_3}{R_T^{1/6}(T^{0\prime}+mc^{0\prime}(z_0))}e^{-\lambda_n(z_0-z_I)}$$
$$\times\left[1+\frac{m_2(1-m\frac{\alpha}{\beta})\left\{1-e^{(p_1-p_2)(z_2-z_0)}\right\}}{(p_1+m_1-m_2-(p_2+m_1-m_2)e^{(p_1-p_2)(z_2-z_0)})}\right]. \quad (212)$$

Notice that in putting an upper limit ∞ in the summation in (212), we have to go through an intermediate analysis where we replace the upper limit by N_1, where $N_1 >> 1$ but smaller than any power of R_T since such a limitation is needed for the validity of (159) used in deriving (207) and (208). The contribution to the summation for λ_n even larger is transcendentally small, as argued earlier. Now since N_1 is far larger than unity and the series in (212) is convergent, the leading order asymptotics is indeed the same as with N_1 replaced by ∞. From (44), (100) and (202), radial segregation in the solid at the interface is

$$\frac{\partial c_s}{\partial r}(r,z_0) \sim \sum_{n=1}^{\infty}\frac{J_1(\lambda_n r)}{\lambda_n^{1/3}J_0(\lambda_n)}\frac{4\epsilon\beta_3(kc^{0\prime}(z_0)-c_s^{0\prime}(z_0))}{R_T^{1/6}(T^{0\prime}+mc^{0\prime}(z_0))}e^{-\lambda_n(z_0-z_I)}$$
$$\times\left[1+\frac{m_2(1-m\frac{\alpha}{\beta})\left\{1-e^{(p_1-p_2)(z_2-z_0)}\right\}}{(p_1+m_1-m_2-(p_2+m_1-m_2)e^{(p_1-p_2)(z_2-z_0)})}\right]$$
$$+\sum_{n=1}^{\infty}\frac{J_1(\lambda_n r)}{\lambda_n^{1/3}J_0(\lambda_n)}\frac{4\epsilon\beta_3 m_2 k\alpha e^{-\lambda_n(z_0-z_I)}\times\left\{1-e^{(p_1-p_2)(z_2-z_0)}\right\}}{\beta R_T^{1/6}(p_1+m_1-m_2-(p_2+m_1-m_2)e^{(p_1-p_2)(z_2-z_0)})} \quad (213)$$

Now, consider fluid velocities in different regions of the melt. By using (40), (41), (71), (72), (98), (108), (150), (154)-(156), (182), (183), (185) and the asymptotic solution (207)-(208) and simple identities of Bessel functions, we can write the asymptotic expressions for radial and vertical fluid velocities for $|z-z_0| = O(R_T^{-1/6})$ as

$$u \sim -\sum_{n=1}^{\infty}\frac{\kappa R_T^{1/3}\epsilon\beta_3 e^{-\lambda_n(z_0-z_I)}}{\lambda_n^{4/3}J_0(\lambda_n)T^{0\prime}}\sum_{j=3}^{5}N_j\omega_j e^{\lambda_n^{1/3}R_T^{1/6}\omega_j(z-z_0)}J_1(\lambda_n r) \quad (214)$$

$$w+1 \sim \sum_{n=1}^{\infty} \frac{\kappa R_T^{1/6} \epsilon \beta_3 e^{-\lambda_n(z_0-z_I)}}{\lambda_n^{2/3} J_0(\lambda_n) T^{0\prime}} \sum_{j=3}^{5} N_j e^{\lambda_n^{1/3} R_T^{1/6} \omega_j (z-z_0)} J_0(\lambda_n r) \tag{215}$$

where

$$N_3 = -1 + i\frac{\sqrt{3}}{3} \quad , \quad N_4 = 2, \quad N_5 = -1 - i\frac{\sqrt{3}}{3}$$

This gives a boundary layer at $z = z_0$ where the fluid velocity changes rapidly. Of course, the numbers N_j are such that at the interface $z = z_0$, each of these expressions reduce to $u = 0$, $w = -1$. Note that the expressions (214) and (215) imply that the velocities change rapidly within a boundary layer that scales as $R_T^{-1/6}$. Aside from the factor $\epsilon\beta_3$, which generally depends on n and the heat transfer parameters, it is easily seen that within the boundary layer, the dimensionless horizontal velocity u scales approximately as $\frac{\kappa R_T^{1/3}}{T^{0\prime}} e^{-\lambda_1(z-z_0)}$, while the vertical nondimensional fluid velocity $w+1$ scales approximately as $\frac{\kappa R_T^{1/6}}{T^{0\prime}} e^{-\lambda_1(z-z_0)}$. The form (214) and (215) suggests that there will be skinny convection cells within this boundary layer. More detailed discussions on the parameter dependence of velocities will be taken up in section 7.

Now, let's consider the neighborhood of $z = z_{II}$, the end of the insulation zone in the melt. We first consider $z < z_{II}$. Since prior analysis shows that for $j = 6, 7, 8$, each of Z_j and therefore C_j is at best $O(1)$, it follows that $C_j e^{W_j(z_{II})}$ is transcendentally small. Thus, from (153), (174), (178), (183) and (C15), it follows that for $j = 6, 7, 8$,

$$e^{W_j(z_{II})} \tilde{C}_j \sim \sum_{k=1}^{8} H_{j,k} R_k \sim H_{j,3} \gamma^5 c_{np}(z_{II})) \sim \gamma^5 H_{j,3} \frac{\lambda_n[-q_1 T^0(z_{II}) + q_2]}{\lambda_n^2 R_T + \lambda_n^6}, \tag{216}$$

where to the leading order, it is known that $H_{j,3} = O(1)$. Further, since Z_j for $j = 3, 4, 5$ turned out $O(1)$ at best, it follows that for $j = 3, 4, 5$, $\tilde{C}_j e^{W_j(z_{II})}$ will be transcendentally small. Thus, in the expression (150), for the stream function coefficient, the leading order contribution comes only from $j = 6, 7, 8$ when $z < z_{II}$ with $|z - z_{II}|$ small enough to be inside the boundary layer (actually an internal layer). It is clear from (150) that

$$c_n \sim \sum_{j=6}^{8} e^{\gamma_j(z-z_{II})} H_{j,3} \gamma^5 c_{np}(z_{II})) \sim \sum_{j=6}^{8} H_{j,3} \frac{\lambda_n[-q_1 T^0(z_{II}) + q_2]}{\lambda_n^2 R_T + \lambda_n^6} e^{\gamma_j(z-z_{II})}$$

Therefore, from (98) and (108),

$$\epsilon\psi \sim \sum_{n=1}^{\infty} J_1(\lambda_n r) \frac{2\lambda_n \kappa R_T \epsilon[-q_1 T^0(z_{II}) + q_2]}{J_0(\lambda_n)(\lambda_n^2 R_T + \lambda_n^6) T^{0\prime}} \sum_{j=6}^{8} H_{j,3}\, e^{\gamma_j(z-z_{II})} \tag{217}$$

Here, unlike what happens near $z = z_0$, most of the contribution to the summation occurs when $\lambda_n = O(R_T^{1/4}) >> 1$. In that case γ_j determined from (158) scales as $R_T^{1/4}$ and hence

from (71) and (72), we conclude that there is a layer that extends downwards from $z = z_{II}$ of thickness $R_T^{-1/4}$, where the radial velocity u scales as

$$\frac{\epsilon\kappa R_T^{1/4}[-q_1 T^0(z_{II}) + q_2]}{T^{0\prime}} \tag{218}$$

and the vertical fluid velocity, $w + 1$ away from $r = 1$ scales as

$$\frac{\epsilon\kappa[-q_1 T^0(z_{II}) + q_2]}{T^{0\prime}} \tag{219}$$

Near the corner, where each of $1 - r$ and $z - z_{II}$ is $O(R_T^{-1/4})$, the vertical velocity also scales as in (218), i.e. it is large as gravity effects become large. Similar arguments for $z > z_{II}$ can be advanced to show that there is also a $R_T^{-1/4}$ boundary layer that extends upwards of $z = z_{II}$ where horizontal velocities scale as in (218) and vertical fluid velocities scale as (219). Within this $R_T^{-1/4}$ layer around $z = z_{II}$, there are convection rolls that can be deduced from the r and z dependence in (217). We can put forward arguments near $z = z_2$ as well to show that there is a similar boundary layer where convection occurs.

Away from these boundary layers at $z = z_0$, $z = z_{II}$ and $z = z_2$, the horizontal and vertical fluid velocity components for $z > z_{II}$ scale as $\frac{\kappa}{T^{0\prime}}$, as can be deduced from (98), (108), (146) and (153). This stays $O(1)$ as with increasing gravity effects. However, there is in this case also a boundary layer near $r = 1$ of thickness $R_T^{-1/4}$ where the vertical velocity scales as $\frac{R_T^{1/4}\kappa}{T^{0\prime}}$ and therefore intensifies with increasing gravity.

For $z < z_{II}$, but away from boundary layers at $z = z_{II}$ and $z = z_0$, it follows from (150) and the behavior (155), (156) of F_j^c for $j = 3, ...8$ that these only gives transcendentally small contribution to c_n. The only sizable contribution comes from possibly $\tilde{C}_1$ and $\tilde{C}_2$, which are determined in (208). Thus, it follows that in this region, the fluid velocity scales at best as $\frac{\kappa}{T^{0\prime}R_T^{1/6}}$ and is reduced by increasing gravity. Unlike the core region for $z > z_{II}$ there is no boundary layer in this case at the side walls near $r = 1$.

In order for our leading order analysis to be self consistent, it is not necessary that scaled fluid velocities u and $w + 1$ be much smaller than unity. Indeed, we obtain the same leading order result if the advection term $\vec{v} \cdot \nabla\vec{v}$ were totally dropped in (3). In order for us to be able to linearize everywhere in the fluid field, it is necessary that the Reynolds number based on the largest fluid velocity $Re_f << 1$. Based on the estimates of the velocities in the boundary layers at $z = z_0$ and $z = z_{II}$, this would require that each of

$$\frac{\kappa R_T^{1/3}\epsilon\beta_3 e^{-\lambda_1(z_0 - z_I)}}{\nu T^{0\prime}} << 1 \tag{220}$$

$$\frac{\kappa R_T^{1/4}\epsilon[-q_1 T^0(z_{II}) + q_2]}{\nu T^{0\prime}} << 1 \tag{221}$$

For the complete validity of our analysis, ϵ needs to be small enough so that both conditions (220) and (221) are met. In addition, we need that the interfacial slope, as given in (212), is all. The latter does not limit ϵ particularly since for larger gravity levels, as on earth, this quantity is small for most experimental conditions without ϵ being small.

Equations (212) and (213) are general results on interfacial deformation and radial segregation that are valid whenever $|R_c| << R_T^{5/6}$ provided the constraints listed in table (2) are satisfied. However, this result is complicated by the dependence through effective parameters β_3, m_1, m_2, which in turn are complicated functions of other parameters. It is therefore instructive to look at a special limit that is applicable to many experimental set up.

6.1 Special case of $D_s/z_0 << 1$ and $\lambda_1(z_2 - z_0)$, $\lambda_1 z_I$, $\lambda_1 z_0 >> 1$

In this case, as mentioned in section 2, $c_i \sim \frac{1}{k}c_2$, $c_s^{0'}$ and its derivatives negligible at $z = z_0$, $c^{0'}(z_0) \sim -(\frac{1}{k} - 1)\frac{c_2}{D}$, $c^{0''}(z_0) \sim (\frac{1}{k} - 1)\frac{c_2}{D^2}$. Therefore, from (134)-(136),

$$\beta_3 \sim -\frac{\kappa_s}{\kappa}\left[(q_{1_s}T_s^0(z_I) - q_{2_s}) - \frac{q_{1_s}}{\lambda_n}T_s^{0'}\right]$$

$$m_1 \sim \frac{(1-k)}{D} - \frac{m(1-k)c_2}{D^2\left(T^{0'} - \frac{mc_2}{D}(\frac{1}{k} - 1)\right)},$$

$$m_2 \sim -\frac{\beta(1-k)c_2}{\alpha D^2\left(T^{0'} - \frac{mc_2}{D}(\frac{1}{k} - 1)\right)}.$$

Thus, in this case the interfacial slope expression (212) reduces to

$$\frac{\partial f}{\partial r} \sim -\sum_{n=1}^{\infty}\frac{4J_1(\lambda_n r)\delta_1}{\lambda_n^{1/3}J_0(\lambda_n)}\left[1 - \frac{\delta_2}{\lambda_n}\right]e^{-\lambda_n(z_0 - z_I)}\left\{\frac{\frac{1}{2D} + \sqrt{\frac{1}{4D^2} + \lambda_n^2} - \frac{1-k}{D}}{\frac{1}{2D} + \sqrt{\frac{1}{4D^2} + \lambda_n^2} - \frac{1-k}{D} - \delta_3}\right\}, \tag{222}$$

where

$$\delta_1 = \frac{\kappa_s\epsilon[q_{1_s}T_s^0(z_I) - q_{2_s}]}{R_T^{1/6}\kappa[T^{0'} - (\frac{1}{k} - 1)\frac{mc_2}{D}]}, \tag{223}$$

$$\delta_2 = \frac{q_{1_s}T_s^{0'}}{[q_{1_s}T_s^0(z_I) - q_{2_s}]}, \tag{224}$$

$$\delta_3 = \frac{\beta(1-k)c_2(1 - \frac{m\alpha}{\beta})}{\alpha D^2(T^{0'} - (\frac{1}{k} - 1)mc_2/D)}. \tag{225}$$

The expression (213) for radial segregation in the crystal at the interface becomes

$$\frac{\partial c_s}{\partial r}(z_0, r) \sim -c_2\frac{(1-k)}{D}\frac{\partial f}{\partial r} - \sum_{n=1}^{\infty}\frac{4J_1(\lambda_n r)}{\lambda_n^{1/3}J_0(\lambda_n)}e^{-\lambda_n(z_0 - z_I)}\frac{\delta_4\delta_1\left[1 - \frac{\delta_2}{\lambda_n}\right]}{(\frac{1}{2D} + \sqrt{\frac{1}{4D^2} + \lambda_n^2} - \frac{1-k}{D} - \delta_3)}, \tag{226}$$

where

$$\delta_4 = \frac{k}{D^2}(1-k)c_2, \tag{227}$$

Each of (222) and (226) can readily be integrated with respect to r since the integral of $J_1(\lambda_n r)$ is $-J_0(\lambda_n r)/\lambda_n$. This readily gives expression for the interfacial shape $f(r)$ and concentration in the solid at the interface $c_s(z_0, r)$.

We now turn to finding simplified expressions for the velocities near the $R_T^{-1/6}$ boundary layer at $z = z_0$ for the simplified case of this subsection. Using (214), (215) and simplified expression for β_3, we obtain that each mode, i.e. coefficient of $J_1(\lambda_n r)$ for the horizontal fluid velocity u scales as

$$\frac{\kappa_s R_T^{1/3}}{\lambda_n^{4/3} J_0(\lambda_n) T^{0\prime}} e^{-\lambda_n(z_0 - z_I)} \epsilon [q_{1s} T_s^0(z_I) - q_{2s}] \, [1 - \frac{\delta_2}{\lambda_n}]. \tag{228}$$

The coefficient of $J_0(\lambda_n r)$ in such a series representation for the vertical fluid velocity $w + 1$ scales as

$$\frac{\kappa_s R_T^{1/6}}{\lambda_n^{2/3} T^{0\prime}} e^{-\lambda_n(z_0 - z_I)} \epsilon [q_{1s} T_s^0(z_I) - q_{2s}] \, [1 - \frac{\delta_2}{\lambda_n}]. \tag{229}$$

7 Discussion of Results and Conclusion

This is a problem with many non-dimensional parameters, as seen in Table 1. It is interesting to note that as $R_T \to \infty$, the leading order asymptotic behavior for the interfacial slope and radial segregation contain far fewer parameters, as seen in (212) and (213). However, in applying this formulae, it should be pointed out that the next order correction in the result is $O(R_c/R_T)$ or $O(R_T^{-1/3})$, which ever is larger.

To the leading order, we find that the interfacial slope and radial segregation scale as $R_T^{-1/6}$, when other parameters are held fixed. Thus, in qualitative agreement with numerical results of Chang & Brown[16], we find that moderately large gravity is worse than large gravity when it comes to controlling interfacial slope and radial segregation.

To avoid a very detailed discussion of all the physical parameter dependence through m_1, m_2 and β_3, we now restrict ourselves to the special case in subsection 6.1. It appears that most experiments satisfy the additional restriction placed in subsection 6.1 so there is not much loss of generality in doing so.

The first notable observation is the crucial dependence of interfacial properties on the quantity $z_0 - z_I$. This is so in the general case, where (212) and (213) hold, as well as in the special case where (222), (226), (228) and (229) hold. Physically, $z_0 - z_I$ is the ratio of the distance of the interface from the end of the insulation zone in the solid to the radius of the cylinder. Since the smallest λ_n is $\lambda_1 = 3.83$, it is clear that an arrangement that

would make $z_0 - z_I$ (note z_0 here is determined from (37) when $St << \kappa/z_2$) a moderately large number, say 2, will ensure that $e^{-\lambda_n(z_0-z_I)}$ is at best $e^{-6.86}$, which is rather small. Since $\lambda_2 = 7.016$ and other λ_n even larger, it is clear that under most such experimental conditions, the dominant contribution to the series (214), (215), (222) and (226) will come from the $n = 1$ term. The profile of each of the interface $f(r)$ and concentration of solute $c_s(r)$ will each look like $J_0(\lambda_1 r)$. In this context, it is interesting to note that we found that the numerically computed Chang & Brown[16] interface for the largest thermal Rayleigh number quoted in their paper is in good agreement with a $J_0(\lambda_1 r)$ profile even when their numerical calculations deal with the fully nonlinear flow. The coefficients however could not be matched as their boundary conditions at $r = 1$ is different from ours. Comparison with the Adornato-Brown[17] profiles is not as favorable, especially near $r = 1$, presumably due to the absence of an ampoule in our analysis. Returning to relations (222), (226), it is clear that if most of the contribution in the series comes from the first term, there will be an approximate proportionality between the radial segration $\frac{\partial c_s}{\partial r}(r, z_0)$ and the interfacial slope $f'(r)$ with the coefficient of proportionality equal to

$$-\frac{(1-k)}{D}c_2\left[1 - \frac{k}{D\left(\frac{1}{2D} + \sqrt{\frac{1}{4D^2} + \lambda_1^2} - \frac{1-k}{D}\right)}\right]. \tag{230}$$

Earlier, Coriell & Sekerka[22] hypothesized such a relation based on a purely diffusive calculation. Brattkus & Davis[21], without any insulation zone, find no necessary relation. We find here that with a proper insulation zone thickness, there is an approximate proportionality between the two though the constant of proportionality in (230) is different from Coriell & Sererka[22] by the appearance of the second term within the square parentheses. Since λ_1 is fairly large, if the Peclet number $\frac{1}{D}$ is not large, then it can be expected that in an approximate way, the second term within the square parentheses in (230) can be replaced by $\frac{k}{D\lambda_1}$, which can again be small for many materials. This may explain why Coriell & Sererka[22] got reasonable agreement with some experiment data.

Now, let us discuss the physical meaning of the scale parameter δ_1 that appears in both (222) and (226). First note from (223) that δ_1 becomes large when

$$T^{0'} - (\frac{1}{k} - 1)mc_2/D \tag{231}$$

approaches zero. However, the term (231) is also present in the denominator of δ_3 in (225). Thus, when the expression (231) approaches zero, both (222) and (226) approach a finite limit. However, the expression (231) has to be kept positive to avoid constitutional supercooling. Indeed, in the absence of capillarity, the condition for the onset of Mullins-Sererka instability of the basic $\epsilon = 0$ state is that the expression in (231) is zero. From the boundary

condition (13b), the quantity $\epsilon[q_1, T_s^0(z_I) - q_2,]$ is the negative of the radial temperature gradient in the solid at $r = 1$, $z = z_I$. Thus, for a dilute alloy, the ratio

$$r_t = \frac{\epsilon[q_1, T_s^0(z_I) - q_2,]}{T^{0\prime} - (\frac{1}{k} - 1)mc_2/D} \tag{232}$$

is approximately the ratio of the horizontal temperature gradients in the solid at $r = 1$, $z = z_I$ to the vertical temperature gradient in the melt. Thus, $\delta_1 = r_t(\kappa_s/\kappa)R_T^{-1/6}$, where κ_s/κ is the ratio of the thermal diffusivities between the solid and the melt.

Now consider the parameter δ_2. It is clearly the z derivative of the log of heat loss rate at $r = 1$, $z = z_I$. If dimensional coordinate $\tilde{z}$ were used, it would be the product of cylinder radius a and the logarithmic derivative with respect to $\tilde{z}$ of the heat loss rate evaluated at the edge of the insulation zone in the solid side. This is clearly a property that can be controlled by appropriate design of the heat transfer properties of the Bridgman apparatus. When most of the contribution of the series in each of (222), (226), (228) and (229), comes from the $n = 1$ term, as is the case with an appropriately large value $z_0 - z_I$, then the special choice

$$\delta_2 = \lambda_1 = 3.83 \tag{233}$$

will have the effect of minimizing the interfacial slope, radial segregation as well as fluid velocities in the boundary layer near the interface. When $\delta_2 < 3.83$, the interface slope in (222) is positive, meaning that the interface will then be bulged towards the solid as reported in previous numerical computations (Chang & Brown[16] for instance).

The role of the parameter δ_3 as defined in (225), is more complex. For sufficiently dilute alloys, clearly since c_2 is small, δ_3 will be small. In that case, the term within the curly parentheses in (222) reduces to unity and therefore in that case there is no explicit dependence of the interfacial shape on the segregation coefficient k or the Peclet number D^{-1} except through δ_1 and $z_0 - z_I$.

Even in a general case, the explicit Peclet number $1/D$ dependence in (222) and (226) is weak, except when Peclet number is comparable or larger than $\lambda_1 = 3.83$

We now discuss fluid motion. As discussed earlier, vigorous fluid motion is confined to the boundary layers near $z = z_0$, $z = z_{II}$ and $z = z_2$ as well as near the side walls $r = 1$ for $z > z_{II}$. Elsewhere, the motion is $O(1)$ in the bulk for $z > z_{II}$ and $o(1)$ for $z < z_{II}$ as gravity is increased. This qualitative feature appears to be in agreement with previous numerical work.

We now discuss details of the motion within the $R_T^{-1/6}$ boundary layer of the interface. Here the scale of the horizontal and vertical fluid velocities for the special case of section 6.1 are given by (228) and (229). Aside from the factor of $(1 - \delta_2/\lambda_n)$, whose significance

has been already discussed, the remaining part of the scale factor, when written in more common notation, as explained in Table 2 is given by

$$\frac{\kappa_s}{\kappa} R_T^{1/3}\ Re^{-1}\ Pr^{-1}\ r_s\ e^{-\lambda_n(z_0-z_I)} \tag{234}$$

for the horizontal velocity u. For the vertical fluid velocity $w+1$, the scale factor is:

$$\frac{\kappa_s}{\kappa} R_T^{1/6}\ Re^{-1}\ Pr^{-1}\ r_s\ e^{-\lambda_n(z_0-z_I)} \tag{235}$$

where $\frac{\kappa_s}{\kappa}$ is the ratio of solid to melt diffusivities, Re is the Reynolds number, Pr is the Prandtl number and the parameter r_s is given by

$$r_s = \frac{\epsilon[q_{1_s} T_s^0(z_I) - q_{2_s}]}{T^{0\prime}} \tag{236}$$

Physically, r_s is the ratio of the horizontal temperature gradient in the solid at $r=1$, $z=z_I$ to the vertical temperature gradient in the melt corresponding to the Tiller et al[1] solution. Note r_s differs from r_t due to an additional term in the denominator. The requirement (220) for dropping nonlinear terms in the Navier-Stokes equation can be written as

$$\frac{\kappa_s}{\kappa} R_T^{1/3}\ Pr^{-1}\ r_s\ e^{-\lambda_1(z_0-z_I)} \ << \ 1 \tag{237}$$

However, we are of the belief that (237) is too stringent since within the boundary layer, the extra z derivative in the Stokes operator part of the Navier-Stokes equation introduces a factor that scales as $R_T^{1/6}$ which only needs to be larger than the convective terms, whose relative size is given by the left hand side of (237). This will have to be confirmed by a nonlinear analysis in the future. Nonetheless, it seems that through a safe choice of $(z_0 - z_I)$, the requirement (236) could perhaps be met in experiment. Of course, $z_0 - z_I$ cannot be chosen arbitrarily large since large temperature gradients have to be maintained to avoid supercooling.

Now, consider fluid motion within the boundary layer around $z = z_{II}$. The scale of the horizontal velocity in (218) can also be written as

$$R_T^{1/4}\ Re^{-1}\ Pr^{-1}\ r_m, \tag{238}$$

where

$$r_m = \frac{\epsilon[q_1 T^0(z_{II}) - q_2]}{T^{0\prime}} \tag{239}$$

is the ratio of the horizontal temperature gradient at $r=1$, $z=z_{II}$ to the Tiller et al[1] vertical temperature gradient in the melt. The vertical fluid velocities in (219) is smaller than the horizontal in this bounday layer by a factor of $R_T^{1/4}$, except near $r=1$, where the fluid velocity components are of comparable magnitude. The requirement (221) for dropping

nonlinear terms may be harder to satisfy in an experiment, even though there is a smaller power of $\dot{R}_T$ in the scaling compared to (237). This is so because there is no quenching factor $e^{-\lambda_1(z_0-z_I)}$. However, because of the boundary layer structure of the solution, the interaction of the interfacial properties at $z = z_0$ with fluid motion near $z = z_{II}$ or $z = z_2$ is weak. This suggests that one can have a highly nonlinear flow in the bulk of the melt, yet if the fluid Reynold number near $z = z_0$ is not large, i.e. (237) holds, then the asymptotic results (222) and (226) will also hold. In that case, it would be interesting to see if the condition (233) can be implemented through appropriate design of the Bridgman apparatus.

Again, because of the boundary layer structure (i.e. exponential decay of the modes away from the boundary) of this problem, as it would be true for any thermally or solutally stabilized configuration, introduction of nonlinearity, when important, is expected to be mathematically manageable since by scaling the $z - z_0$ by $R_T^{1/6}$ and using the scale information on velocities, a nonlinear boundary layer equation with only a few parameters can be formulated. Through appropriate matching with the linear solution in the nearly stagnant core of the insulated zone, a global solution can presumably be constructed. This will be subject of further investigation.

Acknowledgement

First, I would like to acknowledge the help from the referees for pointing out serious deficiencies of the earlier manuscript and also pointing out some significant errors. I also wish to thank Dr. Archie Fripp of NASA Langley Research center for introducing me to the problem and for encouragement during the course of this work.

REFERENCES

1. W.A. Tiller, K.A. Jackson, J.W. Rutter, & B. Chalmers, (1953), The redistribution of solute atomes during solidification of metals, Acta Metallurgica, 1, 428.

2. R. A. Brown, (1988), *AICHE J.* **34**, 881.

3. S.R. Coriell, G.B. McFadden, R.F. Sererka (1985), Cellular Growth During Directional Solidification, *Ann. Rev. Mater. Sci.* , **15**, 119.

4. M. E. Glicksman, S.R. Coriell, G.B. McFadden (1986), *Ann. Rev. Fl. Mech.*, **18**, 307.

5. S. H. Davis (1990), Hydrodynamic interactions in directional solidification, *J. Fluid Mech.*, **212**, 241.

6. H. Nguyen Thi, B. Billia & H. Jamgotchian (1989), Influence of thermosolutal convection on the solidification front during upwards solidification, *J. Fluid Mech.*, **204**, 581.

7. R.Z. Guerin, B. Billia, P. Haldenwang, B. Roux (1988), Solutal convection during directional solidification of a binary alloy: Influence of side walls, *Phys. Fluids.*, **31** , 2086.

8. D.T.J. Hurle, E. Jakeman, A.A. Wheeler (1982), *J. Crys. Growth*, **58**, 163.

9. B. Caroli, C. Caroli, C. Misbah, B. Roulet (1985), *J. Phys.* (Paris), **46**, 1657.

10. D. R. Jenkins (1985), *IMA J. Applied Math*, 35, 145.

11. D.S. Riley & S.H. Davis (1990), *Siam J. Applied Math*, 52, 1.

12. S.H. Davis, U. Muller, C. Dietsche (1984), *J. Fluid Mech.*, 144, 133, 1984.

13. S.H. Coriell, M.R. Cordes, W.J. Boettinger, R.F. Sererka, J. Crystal Growth, 49, 13 (1980), *J. Crystal Growth*, 49, 13 (1980).

14. G.B. McFadden & S.H. Coriell, (1988), *Proc. 1st Nat. Fl. Dynamic Conf.*, Cincinnati (AIAA, Washington, D.C), 1572.

15. M. D. Impey, D.S. Riley, A.A. Wheeler, K.H. Winters, Bifurcation analysis of solutal convection during directional solidification (1991), *Phys. Fluids A.*, **3**, 535.

16. C.J. Chang & R.A. Brown (1983) "Radial Segregation Induced by Natural Convection and Melt/Solid Interface Shape in Vertical Bridgman Growth", *Journal of Crystal Growth* **63**, 343-364.

17. P.M. Adornato & R.A. Brown, (1987), *Journal of Crystal Growth*, **80**, 155.

18. D.H. Kim, & R.A. Brown, (1989), *Journal of Crystal Growth*, **96**, 609.

19. R. A. Brown & D. H. Kim, (1991), "Modelling of directional solidification: from Scheil to detailed numerical simulation ", *Journal of Crystal Growth* **109**, 50-65.

20. E. Scheil, Z. Matallk., 34 (1942), 70.

21. K. Brattkus & S.H. Davis, (1988) "Directional Solidification With Heat Losses", *Journal of Crystal Growth* **91**, 538-556.

22. S. R. Coriell, & R.F. Sererka, (1979), J.Crystal Growth 46, 479.

Appendix A: Derivation of effective interfacial boundary conditions

The purpose of this Appendix is to to derive effective boundary conditions on the melt variables at $z = z_0$ by using (105), (128), (118) and (119) together with the interfacial conditions (120)-(124).

First, recalling that T_s^0 is a linear function as in (35), it is clear from (128) that for $0 < z < z_I$,

$$a_{sn}(z) = a_{snp}(z) + B_1 e^{\lambda_n(z-z_I)} + B_2 e^{-\lambda_n(z-z_I)}, \tag{A1}$$

where

$$a_{snp}(z) = -\frac{1}{\lambda_n}[-q_{1s}T_s^0 + q_{2s}]. \tag{A2}$$

In the insulated zone $z_I < z < z_0$, on the other hand,

$$a_{sn}(z) = \tilde{B}_1 e^{\lambda_n(z-z_I)} + \tilde{B}_2 e^{-\lambda_n(z-z_I)}. \tag{A3}$$

The continuity of a_{sn} and its first derivative at $z = z_I$ implies that each of $\tilde{B}_1$ and $\tilde{B}_2$ can be expressed in terms of B_1 and B_2. Further, from (118), B_2 can be solved in terms of B_1. Going through the algebra, we find the following expression for a_{sn} in the insulated zone $z_I < z < z_0$:

$$a_{sn}(z) = \left(e^{\lambda_n(z-z_I)} - e^{-2\lambda_n z_I} e^{-\lambda_n(z-z_I)}\right) B_1 + G_1 e^{\lambda_n(z-z_I)} + G_2 e^{-\lambda_n(z-z_I)} - a_{snp}(0) e^{-\lambda_n z_I} e^{-\lambda_n(z-z_I)}, , \tag{A4}$$

where

$$G_1 = \frac{1}{2}\left[a_{snp}(z_I) + \frac{a'_{snp}(z_I)}{\lambda_n}\right], \tag{A5}$$

$$G_2 = \frac{1}{2}\left[a_{snp}(z_I) - \frac{a'_{snp}(z_I)}{\lambda_n}\right]. \tag{A6}$$

Using (A4) for $a_{sn}(z_0)$ and $a'_{sn}(z_0)$ and eliminating B_1 between them, we obtain

$$a'_{sn}(z_0) - X_1 a_{sn}(z_0) = Y_1 \tag{A7}$$

where

$$X_1 = \lambda_n \frac{(1 + e^{-2\lambda_n z_0})}{(1 - e^{-2\lambda_n z_0})} \tag{A8}$$

$$Y_1 = 2\lambda_n e^{-\lambda_n(z_0 - z_I)} \frac{\left\{-G_2 + a_{snp}(0) e^{-\lambda_n z_I} - G_1 e^{-2\lambda_n z_I}\right\}}{1 - e^{-2\lambda_n z_0}}. \tag{A9}$$

Similarly, the linear homogeneous equation (105) with condition (119) can be solved in terms of one arbitrary constant. By eliminating this constant between $b'_{sn}(z_0)$ and $b_{sn}(z_0)$, we find

$$b'_{sn}(z_0) - X_2 b_{sn}(z_0) = 0 \tag{A10}$$

where

$$= \frac{p_3 - p_4 e^{z_0(p_4 - p_3)}}{1 - e^{z_0(p_4 - p_3)}}, \tag{A11}$$

where

$$p_3 = -\frac{1}{2D_s} + \sqrt{\frac{1}{4D_s^2} + \lambda_n^2}, \tag{A12}$$

$$p_4 = -\frac{1}{2D_s} - \sqrt{\frac{1}{4D_s^2} + \lambda_n^2}. \tag{A13}$$

From (120)-(122) (with $d_0 = 0$), we can express

$$d_n = -\frac{a_{sn}(z_0) + \frac{m\alpha}{k\beta} b_{sn}(z_0)}{T_s^{0\prime} + mc_s^{0\prime}(z_0)} = -\frac{a_n(z_0) + \frac{m\alpha}{\beta} b_n(z_0)}{T^{0\prime} + mc^{0\prime}(z_0)}. \tag{A14}$$

Equation (120) then becomes

$$a_n(z_0) = n_{11} a_{sn}(z_0) + n_{12} b_{sn}(z_0), \tag{A15}$$

where

$$n_{11} = 1 - \frac{T_s^{0\prime} - T^{0\prime}}{T_s^{0\prime} + \frac{m}{k} c_s^{0\prime}(z_0)}, \tag{A16}$$

$$n_{12} = -\frac{m\alpha \left[T_s^{0\prime} - T^{0\prime}\right]}{k\beta \left[T_s^{0\prime} + \frac{m}{k} c_s^{0\prime}(z_0)\right]}. \tag{A17}$$

From (122) and (A14), we get

$$b_n(z_0) = n_{21} a_{sn}(z_0) + n_{22} b_{sn}(z_0), \tag{A18}$$

where

$$n_{21} = \frac{\beta \left[c^{0\prime}(z_0) - \frac{1}{k} c_s^{0\prime}(z_0)\right]}{\alpha \left[T_s^{0\prime} + \frac{m}{k} c_s^{0\prime}(z_0)\right]}, \tag{A19}$$

$$n_{22} = \frac{1}{k} + \frac{m \left[c^{0\prime}(z_0) - \frac{1}{k} c_s^{0\prime}(z_0)\right]}{k \left[T_s^{0\prime} + \frac{m}{k} c_s^{0\prime}(z_0)\right]}. \tag{A20}$$

Thus,

$$a_{sn}(z_0) = \frac{n_{22} a_n(z_0) - n_{12} b_n(z_0)}{n_{22} n_{11} - n_{12} n_{21}}, \tag{A21}$$

$$b_{sn}(z_0) = \frac{-n_{21} a_n(z_0) + n_{11} b_n(z_0)}{n_{22} n_{11} - n_{12} n_{21}}. \tag{A22}$$

Further, from the simplification of (123) into $a'_{sn}(z_0) = \frac{\kappa}{\kappa_s} a'_n(z_0)$ (due to linearity of T_s^0 and T^0) and (A7) and (A21), it follows that

$$\frac{a'_n(z_0)}{\lambda_n} + \beta_1 a_n + \beta_2 b_n = \frac{\beta_3}{\lambda_n} e^{-\lambda_n (z_0 - z_I)}, \tag{A23}$$

where

$$\beta_1 = -\frac{X_1 \kappa_s n_{22}}{\lambda_n \kappa (n_{22} n_{11} - n_{12} n_{21})} \tag{A24}$$

$$\beta_2 = \frac{X_1 \kappa_s n_{12}}{\lambda_n \kappa (n_{22} n_{11} - n_{12} n_{21})} \tag{A25}$$

$$\beta_3 = \frac{2\lambda_n \kappa_s \left[-G_2 + a_{snp}(0) e^{-\lambda_n z_I} - G_1 e^{-2\lambda_n z_I}\right]}{\kappa \left[1 - e^{-2\lambda_n z_0}\right]} \tag{A26}$$

Using expressions for n_{11}, n_{12}, n_{21}, n_{22}, X_1, G_1 and G_2 in the above and carrying out the algebra, we get

$$\beta_1 = -\frac{\kappa_s (T_s^{0'} + mc^{0'}(z_0))(1 + e^{-2\lambda_n z_0})}{\kappa (mc^{0'}(z_0) + T^{0'})(1 - e^{-2\lambda_n z_0})}, \tag{A27}$$

$$\beta_2 = -\frac{\kappa_s m \alpha (T_s^{0'} - T^{0'})(1 + e^{-2\lambda_n z_0})}{\kappa \beta (mc^{0'}(z_0) + T^{0'})(1 - e^{-2\lambda_n z_0})} \tag{A28}$$

$$\beta_3 = -\frac{\kappa_s \left\{(q_{1_s} T_s^0(z_I) - q_{2_s})(1 + e^{-2\lambda_n z_I}) - 2(q_{1_s} T_s^0(z_I) - q_{2_s}) e^{-\lambda_n z_I} - \frac{q_{1_s}}{\lambda_n} T_s^{0'}(1 + e^{-2\lambda_n z_I})\right\}}{\kappa \left[1 - e^{-2\lambda_n z_0}\right]}, \tag{A29}$$

Using (124), (A14), (A22), we obtain another effective boundary condition for the melt variables of the form

$$b_n'(z_0) + m_1 b_n(z_0) + m_2 a_n(z_0) = 0, \tag{A30}$$

where

$$m_1 = \beta_4 + X_2 \beta_5, \tag{A31}$$

$$m_2 = \beta_6 + X_2 \beta_7 \tag{A32}$$

In the above,

$$\beta_4 = -\frac{k-1}{D} + \frac{m\left(\frac{D_s}{D} c_s^{0''}(z_0) + \frac{(k-1)}{D} c^{0'}(z_0) - c^{0''}(z_0)\right)}{(T^{0'} + mc^{0'}(z_0))} \tag{A33}$$

$$\beta_5 = -\frac{D_s n_{11}}{D(n_{11} n_{22} - n_{12} n_{21})} \tag{A34}$$

$$\beta_6 = \frac{\beta\left(\frac{D_s}{D} c_s^{0''}(z_0) + \frac{(k-1)}{D} c^{0'}(z_0) - c^{0''}(z_0)\right)}{\alpha (T^{0'} + mc^{0'}(z_0))} \tag{A35}$$

$$\beta_7 = \frac{D_s n_{21}}{D(n_{11} n_{22} - n_{12} n_{21})} \tag{A36}$$

Using expressions for n_{11}, n_{12}, n_{21} and n_{22} in the above, the expressions for β_5 and β_7 simplify to:

$$\beta_5 = -\frac{D_s \left(mc_s^{0'}(z_0) + kT^{0'}\right)}{D(mc^{0'}(z_0) + T^{0'})}, \tag{A37}$$

$$\beta_7 = \frac{D_s\beta\left(kc^{0'}(z_0) - c_s^{0'}(z_0)\right)}{D\alpha(mc^{0'}(z_0) + T^{0'})}. \qquad (A38)$$

Equations (A23) and (A30) form the effective boundary conditions on the melt variables that incorporates all the the coupling between the variables on the solid and melt side.

Appendix B: Derivation of the asymptotic form of approximate general solution

The purpose of this Appendix is to find approximate expression for c_{np}, a_{np}, b_{np}, F_j^c, F_j^b and F_j^a appearing in (146)-(152) $R_T >> 1$ with $|R_c| << R_T$.

It is possible to find uniformly valid asymptotic representation of the solution for all λ_n in this limit. Nonetheless, this expression is too complicated and not very suitable for algebraic manipulation when $R_c << R_T^{5/6}$. So, we first derive easier expressions for the asymptotic behavior of the solution for $R_T >> 1$ and $\lambda_n^2|R_c| << (\lambda_n^2 R_T)^{5/6}$. Clearly, even when $|R_c| << R_T^{5/6}$, this condition is not uniformly valid for all λ_n. Thus, for large enough λ_n, we have to use the more general expression; nonetheless, from the arguments in section 6, we know that the detailed behavior of the solution for large λ_n is not necessary to conclude that the contribution to the series (96)-(101) from large λ_n is indeed negligible and so the behavior of the solution for $|R_c| < R_T^{5/6}$ can be deduced from the results in the following subsection

B1. Subcase $\lambda_n^2|R_c| << \gamma^5$, $R_T >> 1$

From (143), in the heat zone $z_{II} < z < z_0$, we have

$$\left[\mathcal{L}_1\mathcal{L}_2\mathcal{L}_3 + \lambda_n^2 R_c \mathcal{L}_1 h(z) - \lambda_n^2 R_T \mathcal{L}_2\right] c_n = \mathcal{L}_2\left[-\lambda_n(-q_1 T^0 + q_2)\right]. \tag{B1}$$

To the leading order, we expect

$$c_n \sim c_n^0, \tag{B2}$$

where c_n^0 satisfies

$$\left[\mathcal{L}_1\mathcal{L}_2\mathcal{L}_3 - \lambda_n^2 R_T \mathcal{L}_2\right] c_n = \mathcal{L}_2\left[-\lambda_n(-q_1 T^0 + q_2)\right]. \tag{B3}$$

Thus, we can write

$$\left[\mathcal{L}_1\mathcal{L}_3 - \lambda_n^2 R_T\right] c_n = -\lambda_n[-q_1 T^0 + q_2] + \sum_{j=1}^{2} \gamma^{-2}\left\{L_1[p_j]L_3[p_j] - \lambda_n^2 R_T\right\} A_j e^{p_j(z-z_0)} \tag{B4}$$

where A_1, A_2 are arbitrary constants and

$$\gamma = \lambda_n^{1/3} R_T^{1/6} \tag{B5}$$

$$L_1[y] = y^2 - \lambda_n^2 \tag{B6}$$

$$L_2[y] = D[y^2 - \lambda_n^2] + y \tag{B7}$$

$$L_3[y] = (y^2 - \lambda_n^2)^2 + \frac{y}{\nu}(y^2 - \lambda_n^2) \tag{B8}$$

$$p_1 = -\frac{1}{2D} - \sqrt{\frac{1}{4D^2} + \lambda_n^2} \tag{B9}$$

$$p_2 = -\frac{1}{2D} + \sqrt{\frac{1}{4D^2} + \lambda_n^2} \tag{B10}$$

On solving (B4), we obtain,

$$c_n^0 = c_{np}^0 + \sum_{j=1}^{2} \gamma^{-2} A_j e^{p_j(z-z_0)} + \sum_{j=3}^{8} A_j e^{\gamma_j(z-z_0)}, \tag{B11}$$

where

$$c_{np}^0 = \frac{\lambda_n[-q_1 T^{\omega} + q_2]}{[\lambda_n^2 R_T + \lambda_n^6]} - \frac{\lambda_n^5 q_1 T^{\omega'}}{\nu[\lambda_n^2 R_T + \lambda_n^6]^2}, \tag{B12}$$

and γ_j are the six independent roots of

$$L_3[\gamma_j] L_1[\gamma_j] - \lambda_n^2 R_T = 0 \tag{B13}$$

that are labelled such that for $R_T >> \lambda_n^4$,

$$\gamma_j \sim \gamma\omega_j \tag{B14}$$

where ω_j are the six roots of unity defined by

$$\omega_3 = -e^{i\pi/3} = -\omega_8 \tag{B15}$$

$$\omega_4 = -1 = -\omega_7 \tag{B16}$$

$$\omega_5 = -e^{-i\pi/3} = -\omega_6 \tag{B17}$$

In order to find the next order correction in the asymptotic expansion

$$c_n \sim c_n^0 + c_n^1 + \ldots \tag{B18}$$

we notice that c_n^1 satisfies

$$\mathcal{L}_2\left[\mathcal{L}_1\mathcal{L}_3 - \lambda_n^2 R_T\right] c_n^1 = -\lambda_n^2 R_c \mathcal{L}_1[h c_{np}^0] - \lambda_n^2 R_c \gamma^{-2} \sum_{j=1}^{2} A_j L_1[\hat{p}_j] e^{\hat{p}_j(z-z_0)} - \lambda_n^2 R_c \sum_{j=3}^{8} A_j L_1[\hat{\gamma}_j] e^{\hat{\gamma}_j(z-z_0)}, \tag{B19}$$

where

$$\hat{p}_j = p_j - \frac{1}{D}, \tag{B20}$$

$$\hat{\gamma}_j = \gamma_j - \frac{1}{D}. \tag{B21}$$

Then one can solve (B19) in a standard manner to find that

$$c_n^1 = c_{n_p}^1 - \gamma^{-2}\lambda_n^2 R_c \sum_{j=1}^{2} \frac{A_j L_1[\hat{p}_j] f(z) e^{p_j(z-z_0)}}{L_2[\hat{p}_j]\{L_1[\hat{p}_j] L_3[\hat{p}_j] - \lambda_n^2 R_T\}}$$

$$-\lambda_n^2 R_c \sum_{j=3}^{8} \frac{A_j L_1[\hat{\gamma}_j] f(z) e^{\gamma_j (z-z_0)}}{L_2[\hat{\gamma}_j] \{L_1[\hat{\gamma}_j] L_3[\hat{\gamma}_j] - \lambda_n^2 R_T\}} \qquad (B22)$$

where c_{np}^1 is a particular solution of the form

$$c_{np}^1 = (\hat{A}_2(z - z_0) + \hat{A}_1) h(z)$$

that satisfies

$$\mathcal{L}_2 \left[\mathcal{L}_1 \mathcal{L}_3 - \lambda_n^2 R_T\right] c_{np}^1 = -\lambda_n^2 R_c \mathcal{L}_1 [h c_{np}^0].$$

When $R_T >> \lambda_n^4$, the above asymptotes to

$$c_{np}^1 \sim g(z) \frac{R_c}{R_T L_2[-D^{-1}]} \left\{ L_1[-D^{-1}] c_{np}^0 - \frac{2}{D} c_{np}^{0'} + \frac{L_1[-D^{-1}] c_{np}^{0'}}{L_2[-D^{-1}]} \right\} \qquad (B23)$$

Thus, if we write

$$c_n = c_{np} + \sum_{j=1}^{2} \gamma^{-2} C_j F_j^c + \sum_{j=3}^{8} C_j F_j^c \qquad (B24)$$

as in (146), then

$$c_{np} \sim c_{np}^0 + c_{np}^1 + .. \quad .$$

Note that in the special case $R_T << \lambda_n^4$, c_{np} and its derivatives are $O(R_T^{-1})$, which follows from (B12) and (B23). This scaling property is used in section 6. Further, in (B24),

$$F_j^c \sim \frac{p_j}{D} e^{p_j (z - z_{2(j-1)})} \left\{ 1 - \frac{\lambda_n^2 R_c L_1[\hat{p}_j] h(z)}{L_2[\hat{p}_j] [L_1[\hat{p}_j] L_3[\hat{p}_j] - \lambda_n^2 R_T]} + .. \right\} \quad \text{for } j = 1, 2 \ , \qquad (B25)$$

$$F_j^c \sim e^{\gamma_j (z - z_0)} \left\{ 1 - \frac{\lambda_n^2 R_c L_1[\hat{\gamma}_j] h(z)}{L_2[\hat{\gamma}_j] [L_1[\hat{\gamma}_j] L_3[\hat{\gamma}_j] - \lambda_n^2 R_T]} + .. \right\} \quad \text{for } j = 3, 4, 5 \ , \qquad (B26)$$

$$F_j^c \sim e^{\gamma_j (z - z_2)} \left\{ 1 - \frac{\lambda_n^2 R_c L_1[\hat{\gamma}_j] h(z)}{L_2[\hat{\gamma}_j] [L_1[\hat{\gamma}_j] L_3[\hat{\gamma}_j] - \lambda_n^2 R_T]} + .. \right\} \quad \text{for } j = 6, 7, 8 \ , \qquad (B27)$$

where we choose new arbitrary constants

$$C_1 = \gamma^5 A_1, \ C_2 = \gamma^5 A_2 e^{p_2 (z_2 - z_0)}, \ C_j = \gamma^5 A_j \text{ for j} = 3, 4, 5 \ \text{C}_\text{j} = \gamma^5 \text{A}_\text{j} e^{\gamma_j (z_2 - z_0)} \text{ for j} = 6, 7, 8 \qquad (B28)$$

Using (145a), we can solve for a_n once c_n is known. Such a solution also needs to be consistent with (144a). We find that

$$a_n \sim a_{np} + \sum_{j=1}^{8} \gamma^{-1} C_j F_j^a, \qquad (B29)$$

where

$$a_{np} \sim a_{np}^0 + a_{np}^1 + \ldots \ , \qquad (B30)$$

where

$$a^0_{np} = -\frac{\lambda_n^5[-q_1T^0 + q_2]}{\lambda_n^2 R_T + \lambda_n^6} - \frac{\lambda_n^5 q_1 T^{0'}\, R_T}{\nu[\lambda_n^2 R_T + \lambda_n^6]^2} \quad , \tag{B31}$$

and a^1_{np} is a particular solution of the form

$$a^1_{np} = \left[\hat{B}_2(z - z_0) + \hat{B}_1\right] h(z) \tag{B32}$$

that satisfies

$$\mathcal{L}_1 a^1_{np} = -\lambda_n^2 R_T c^1_{np} \, . \tag{B33}$$

When $R_T >> \lambda_n^4$, the expression simplifies so that

$$a^1_{np} \sim -\frac{\lambda_n^2 R_c h(z)}{L_2[-D^{-1}]L_1[-D^{-1}]}\left[L_1[-D^{-1}]c^0_{np} + \frac{L_1[-D^{-1}]}{L_2[-D^{-1}]}c^{0'}_{np}\right] \quad . \tag{B34}$$

Further,

$$F^a_j \sim e^{p_j(z - z_{(2j-2)})}\left[1 - \frac{R_c p_j h(z) L_1[\hat{p}_j]\,(-L_2[\hat{p}_j]L_3[\hat{p}_j] + D\lambda_n^2 R_T)}{D R_T \hat{p}_j L_2[\hat{p}_j]\,(L_1[\hat{p}_j]L_3[\hat{p}_j] - \lambda_n^2 R_T)} + ..\right) \quad \text{for } j = 1,2 \quad , \tag{B35}$$

$$F^a_j \sim -\frac{\gamma^2}{\gamma_j^2 - \lambda_n^2}\, e^{\gamma_j(z - z_0)}\left[1 - \frac{R_c p_j h(z) L_1[\hat{\gamma}_j]\,(-L_2[\hat{\gamma}_j]L_3[\hat{\gamma}_j] + D\lambda_n^2 R_T)}{D R_T \hat{\gamma}_j L_2[\hat{\gamma}_j]\,(L_1[\hat{\gamma}_j]L_3[\hat{\gamma}_j] - \lambda_n^2 R_T)} + ..\right) \quad \text{for } j = 3,4,5 \, , \tag{B36}$$

$$F^a_j \sim -\frac{\gamma^2}{\gamma_j^2 - \lambda_n^2}\, e^{\gamma_j(z - z_2)}\left[1 - \frac{R_c p_j h(z) L_1[\hat{\gamma}_j]\,(-L_2[\hat{\gamma}_j]L_3[\hat{\gamma}_j] + D\lambda_n^2 R_T)}{D R_T \hat{\gamma}_j L_2[\hat{\gamma}_j]\,(L_1[\hat{\gamma}_j]L_3[\hat{\gamma}_j] - \lambda_n^2 R_T)} + ..\right) \quad \text{for } j = 6,7,8 \, . \tag{B37}$$

Using $b_n = -\mathcal{L}_3 c_n - a_n$, we can write

$$b_n = b_{np} + \sum_{j=1}^{2} \gamma^4 C_j F^b_j + \lambda_n^2 R_c \gamma^{-1} \sum_{j=3}^{8} C_j F^b_j \quad , \tag{B38}$$

where

$$b_{np} = -\mathcal{L}_3[c_{np}] - a_{np} \quad . \tag{B39}$$

Simplified expressions are possible for $R_T >> \lambda_n^4$, which we do not care to write. The only property that will be of importance in the analysis in section 6 is that b_{np} is this range of λ_n is $O(R_c/R_T, R_T^{-1})$, as is a_{np}, which follows from (B30), (B31) and (B34).

Further, in the general case in (B38),

$$F^b_j \sim e^{p_j(z - z_{(2j-2)})}\left(-\frac{p_j L_3[p_j]}{D\gamma^6} - 1 - \frac{R_c h(z) L_1[\hat{p}_j] p_j}{R_T \gamma^2 L_2[\hat{p}_j]\hat{p}_j} + ..\right) \quad \text{for } j = 1,2 \quad , \tag{B40}$$

$$F^b_j \sim -e^{\gamma_j(z - z_0)}\frac{\gamma D L_1[\hat{\gamma}_j]}{\hat{\gamma}_j L_2[\hat{\gamma}_j]} h(z) \; + \; .. \; \text{for } j = 3,4,5 \quad , \tag{B41}$$

$$F_j^b \sim -e^{\gamma_j(z-z_2)}\frac{\gamma D L_1[\hat{\gamma}_j]}{\hat{\gamma}_j L_2[\hat{\gamma}_j]}h(z) + .. \text{ for } j = 6,7,8 \qquad (B42)$$

Now, we comment on the validity of the asymptotic behavior given so far. The behavior of the particular solutions a_{np}, b_{np} and c_{np} is clearly valid anytime $|R_c| << R_T$. This is uniformly true for all λ_n. Further, expressions (B25), (B35) and (B40) is also consistent in this regime for all λ_n. However, the expressions (B26) and (B27) do not remain valid when $|\lambda_n^2 R_c|$ is the same order or larger than γ^5, i.e. $(\lambda_n^2 R_T)^{5/6}$. This is because from definition,

$$L_1[\gamma_j]L_3[\gamma_j] = \lambda_n^2 R_T = \gamma^6.$$

Thus, for large R_T,

$$L_1[\hat{\gamma}_j]L_3[\hat{\gamma}_j] = O(\gamma^5).$$

In order that the second term in (B26) and (B27) be smaller than the first term, it is necessary that $|\lambda_n^2 R_c| << \gamma^5$. This is the origin of the restriction for the asymptotic behavior shown thus far. Note that the condition $\lambda_n^2|R_c| << \gamma^5$ cannot be uniformly valid for all λ_n even when $|R_c| << R_T^{5/6}$.

B2. General form of Solution for $|R_c| << R_T$

In order to find uniformly valid expression for all λ_n and at the same time find expressions valid for $|R_c| << R_T$, we find six independent solutions to the associated homogeneous equation in (B1) in the WKB form. These solutions will replace the expressions (B26) and (B27). Once this is found appropriate expressions can easily be found to replace (B36),(B37), (B41) and (B42), which are also invalid in the general case.

We consider WKB solution of the form:

$$F_j^c = e^{W_j} \quad \text{for} \quad j = 3,4..,8 \qquad (B43)$$

We will think of the relation (B43) as exact and relate the WKB approximate behavior through the relation

$$W_j \sim W_{0_j} + W_1, \qquad (B44)$$

We find that for $R_T >> 1$, with $|R_T - R_c| >> 1$, a uniformly valid expression for W_{0_j} is given by the following expressions

$$W_{0_3} = -\int_{z_0}^{z}[(\lambda_n^2 R_T - \lambda_n^2\frac{R_c}{D}h(z))^{\frac{1}{3}}e^{i2\frac{\pi}{3}} + \lambda_n^2]^{\frac{1}{2}}dz \qquad (B45)$$

$$W_{0_4} = -\int_{z_0}^{z}[(\lambda_n^2 R_T - \lambda_n^2\frac{R_c}{D}h(z))^{\frac{1}{3}} + \lambda_n^2]^{\frac{1}{2}}dz \qquad (B46)$$

$$W_{0_5} = -\int_{z_0}^{z}[(\lambda_n^2 R_T - \lambda_n^2\frac{R_c}{D}h(z))^{\frac{1}{3}}e^{-i2\frac{\pi}{3}} + \lambda_n^2]^{\frac{1}{2}}dz \qquad (B47)$$

$$W_{0_6} = \int_{z_2}^{z} [(\lambda_n^2 R_T - \lambda_n^2 \frac{R_c}{D} h(z))^{\frac{1}{3}} e^{-i2\frac{\pi}{3}} + \lambda_n^2]^{\frac{1}{2}} dz \qquad (B48)$$

$$W_{0_7} = \int_{z_2}^{z} [(\lambda_n^2 R_T - \lambda_n^2 \frac{R_c}{D} h(z))^{\frac{1}{3}} + \lambda_n^2]^{\frac{1}{2}} dz \qquad (B49)$$

$$W_{0_8} = \int_{z_2}^{z} [(\lambda_n^2 R_T - \lambda_n^2 \frac{R_c}{D} h(z))^{\frac{1}{3}} e^{i2\frac{\pi}{3}} + \lambda_n^2]^{\frac{1}{2}} dz \qquad (B50)$$

In the above, we proceed with the understanding that the principal argument is being used in taking the squareroots and cube roots. W_{1_j} for $3 \leq j \leq 5$ is determined by

$$W_{1_j} = \int_{z_0}^{z} W'_{1_j}(z) dz \qquad (B51)$$

and W_{1_j} for $6 \leq j \leq 8$, is determined by

$$W_{1_j} = \int_{z_2}^{z} W'_{1_j}(z) dz \qquad (B52)$$

where each W'_{1_j} are determined in terms of the corresponding W'_{0_j} through

$$W'_1 = -\frac{W''_0 \left\{ 27(W_0'^2 - \lambda_n^2)^3 + 24\lambda_n^2 (W_0'^2 - \lambda_n^2)^2 \right\} + \left(\frac{3}{D} + \frac{1}{\nu}\right) W'_0 (W_0'^2 - \lambda_n^2)^3 - \frac{3\lambda_n^2 R_T W'_0}{D}}{6W'_0 (W_0'^2 - \lambda_n^2)^3} \qquad (B53)$$

Further, note that when $R_T >> |R_c|$ with $\lambda_n^4 << R_T$, these expressions reduce to

$$W'_{0_j} \sim \gamma \omega_j \qquad (B56)$$

in agreement with (B14). Thus, the expression (B43) is a generalization of the earlier formulae for F_j^c for $j = 3, 4, ..8$

Now consider, finding F_j^a for $j = 3, 4..8$. It is determined as a particular solution to

$$\mathcal{L}_1 F_j^a = -\lambda_n^2 R_T F_j^c \qquad (B57)$$

Through a standard dominant balance procedure, we obtain for $j = 3, ..8$,

$$F_j^a \sim -\gamma^6 e^{W_j} \left\{ \frac{1}{W_j'^2 - \lambda_n^2} - \frac{W''_j}{(W_j'^2 - \lambda_n^2)^2} + ... \right\} \qquad (B58)$$

Since $F_j^b = -F_j^a - \mathcal{L}_3 F_j^c$, it follows that for $j = 3, 4, ..8$,

$$F_j^b \sim \frac{-1}{W_j'^2 - \lambda_n^2} \left[((W_j'^2 - \lambda_n^2)^3 - \gamma^6 - 2(W_j'^2 - \lambda_n^2)^2 W''_j + 4W_j'^2 W''_j (W_j'^2 - \lambda_n^2) + \frac{W'_j}{\nu} (W_j'^2 - \lambda_n^2)^2 \right] \qquad (B59)$$

Notice that it is necessary to retain all the terms in (B59) even when the first two terms within the parentheses are clearly $O(\gamma^6)$ while the remaining are $O(\gamma^5)$ because there is cancellation between there is cancellation these leading order terms because

$$(W_{0_r}'^2 - \lambda_n^2)^3 - \gamma^6 = \lambda_n^2 \frac{R_c}{D} h(z)$$

and this need not be larger than γ^5. Relations (B43) with asymptotic behavior (B44) and relations (B45)-(B53) replace the more restricted expression (B25) and (B26) when $\lambda_n^2 R_c$ is $O(\gamma^5)$ or larger, provided $R_T >> |R_c|$. The remaining expressions (B25), (B12) remain valid. As far as a_n and b_n, expressions (B57) and (B58) replace (B36)-(B37) and (B41)-(B42) respectively, other expressions (B35), (B30), (B31), (B32), (B39) and (B40) still remain valid as long as $R_T >> |R_c|$.

Appendix C: Asymptotic evaluation of solution to $MZ = S$

The purpose of this Appendix is to carry out the asymptotic evaluation of solution to (184) when $R_T >> 1$ and $\lambda_n = O(1)$. In this case, γ defined by (147) is $>> 1$ and the asymptotic relation (B159) for the roots γ_j hold.

First, we consider the elements P_1 through P_8 that appear in the expression for S in (186). Since for $1 \leq l \leq 4$, the elements $M_{l,k}e^{-W_k(z_{II})}$ scale as $e^{-\gamma_j(z_{II}-z_0)}$ for $j = 6,7,8$ and is therefore transcendentally small in R_T. We ignore such terms in P_l. Similarly, for $5 \leq l \leq 8$, the elements $M_{l,k}e^{-W_k(z_{II})}$ scale as $e^{\gamma_j(z_2-z_{II})}$ for $j = 3,4,5$ and is transcendentally small in R_T. This leaves us with the contribution from terms multiplying $H_{1,j}$ and $H_{2,j}$ in (187) and (188). Thus, it is necessary to calculate the first two rows of the matrix H, which is the inverse of G.

First, consider the simplification of the matrix G, whose elements are defined by (175), (176), (179) and (180). On examination of (153)-(170), it is clear that

$$G \sim G^0 + O\left(\lambda_n^2 R_c \gamma^{-5}\right) , \tag{C1}$$

where for $k = 1,2$,

$$G^0_{k,j} = p_j^{k-1}, \text{ for j} = 1,2, \quad \mathrm{G^0_{k,j}} = -\frac{\gamma\gamma_j^{k-1}}{\gamma_j^2 - \lambda_n^2} \text{ for j} = 3,..8 , \tag{C2}$$

while for $k = 3,..8$,

$$G^0_{k,j} = \frac{p_j^{(k-2)}}{D\gamma^{(k-2)}} \text{ for j} = 1,2, \quad \mathrm{G^0_{k,j}} = \left(\frac{\gamma_j}{\gamma}\right)^{(k-3)} \text{ for j} = 3,..8. \tag{C3}$$

Now consider the problem of determining the the first two rows of $H^0 = G^{0^{-1}}$. This can be conveniently done by finding the first two components X_1^l and X_2^l of the vector X^l that satisfies

$$G^0 X^l = E^l = (0,0,0,,,1,..0)^T , \tag{C4}$$

the only nonzero element of E^l is a one at the l-th entry. It is convenient to define symbols r_k so that

$$L_3[y] = (y^2 - \lambda_n^2)^2 + \frac{y}{\nu}(y^2 - \lambda_n^2) = \sum_{k=0}^{4} r_k y^k \tag{C5}$$

Thus,

$$r_0 = \lambda_n^4 , \; r_1 = -\frac{\lambda_n^2}{\nu} , \; , r_2 = -2\lambda_n^2 , \; r_3 = \frac{1}{\nu} , \; r_4 = 1. \tag{C6}$$

Also, we define $r_k = 0$ for negative k. Notice that (158) implies that

$$\frac{1}{\gamma_j^2 - \lambda_n^2} = \gamma^{-6} L_3[\gamma_j]$$

So, when the first two components of the vector identity (C4) is written long hand, we get

$$X_1^l + X_2^l = \sum_{j=3}^{8} \gamma^{-5} L_3[\gamma_j] X_j^l + \delta_{l,1} = \gamma^{-5} \sum_{k=0}^{4} r_k \sum_{j=3}^{8} \gamma_j^k X_j^l + \delta_{l,1}, \qquad (C7)$$

$$p_1 X_1^l + p_2 X_2^l = \sum_{j=3}^{8} \gamma^{-5} \gamma_j L_3[\gamma_j] X_j^l + \delta_{l,2} = \gamma^{-5} \sum_{k=0}^{4} r_k \sum_{j=3}^{8} \gamma_j^(k+1) X_j^l + \delta_{l,2}\ , \qquad (C8)$$

where $\delta_{k,j}$ is the usual Kronecker delta symbol. From the $(k+3)$-rd element of the vector identity, with k ranging from 0 to 5, it follows that

$$\sum_{j=3}^{8} \gamma_j^k X_j^l = -\frac{1}{\gamma D} \sum_{j=1}^{2} p_j^{k+1} X_j^l + \delta_{k,l-3} \qquad (C9)$$

Using this in (C7) and (C9), we get

$$X_1^l + X_2^l = -\frac{1}{D\gamma^6} \sum_{j=1}^{2} p_j L_3[p_j] X_j^l + \gamma^{-5} r_{l-3} + \delta_{l,1}, \qquad (C10)$$

$$p_1 X_1^l + p_2 X_2^l = -\frac{1}{D\gamma^6} \sum_{j=1}^{2} p_j^2 L_3[p_j] X_j^l + \gamma^{-5} r_{l-4} + \delta_{l,2}. \qquad (C11)$$

from which it follows that

$$H_{1,l}^0 = X_1^l = \left[1 + \frac{p_1}{D\gamma^6} L_3[p_1]\right]^{-1} \left[\frac{p_2 \delta_{l,1} - \delta_{l,2}}{p_2 - p_1} + \gamma^{-5} \frac{(p_2 r_{l-3} - r_{l-4})}{(p_2 - p_1)}\right], \qquad (C12)$$

$$H_{2,l}^0 = X_2^l = \left[1 + \frac{p_2}{D\gamma^6} L_3[p_2]\right]^{-1} \left[\frac{p_1 \delta_{l,1} - \delta_{l,2}}{p_1 - p_2} + \gamma^{-5} \frac{(p_1 r_{l-3} - r_{l-4})}{(p_1 - p_2)}\right]. \qquad (C13)$$

Now, let's consider the other elements $H_{k,l}^0$ for $k \geq 3$. Clearly, from (C9), it follows that that for k ranging from 0 to 5,

$$\sum_{j=3}^{8} \gamma^{-k} \gamma_j^k H_{j,l}^0 = -\gamma^{-k-1} D^{-1} \sum_{j=1}^{2} p_j^{k+1} H_{j,l}^0 + \delta_{k,l-3} \qquad (C14)$$

Using the results (C12) and (C13), it is clear that the right hand side of (C14) is $O(\gamma^{-2})$ for $l = 1, 2$ and $O(1)$ for $l = 3, 4, ...8$. Since the coefficient of each term on the left hand side of (C14) is $O(1)$ in the asymptotic limit $\gamma \rightarrow \infty$, it follows that

$$H_{j,l}^0 = O(\gamma^{-2}) \text{ for } j = 1,2 \text{ and } H_{j,l}^0 = O(1) \text{ for } j = 3, ...8 \qquad (C15)$$

Now, since from (174), (B12), (B30), (B31), (B34), a_{np} and its first derivatives are $O(R_c/R_T, R_T^{-1})$, while c_{np} and its derivatives are $O(R_T^{-1})$, it follows from (174) and (178) that

each of R_1 and R_2 are $O(R_c/R_T, \gamma^{-6})$, while R_3 and R_4 are $O(\gamma^{-1})$, and $O(\gamma^{-2})$ respectively. All other components are $O(\gamma^{-3}$ or smaller. This means that for $j = 1, 2$,

$$\gamma e^{-W_j(z_{II})} \sum_{k=1}^{8} H_{j,k} R_k = e^{-W_j(z_{II})} \times O\left(\gamma^{-5}\lambda_n^2 R_c, \gamma^{-5}\right), \tag{C16}$$

and so

$$P_l = e^{-p_2(z_{II}-z_0)} \times O\left(\gamma^{-5}\lambda_n^2 R_c, \gamma^{-5}\right) \quad \text{for} \quad l = 1,2,3,4 \ . \tag{C17}$$

$$P_l = e^{p_1(z_2-z_{II})} \times O\left(\gamma^{-5}\lambda_n^2 R_c, \gamma^{-5}\right) \quad \text{for} \quad l = 5,6,7,8 \ . \tag{C18}$$

Further, we notice that in (186) in the terms beside P_l, all except S_3 are $O(\gamma^{-5}R_c, \gamma^{-1}) = o(1)$, where as S_3 contains a term that scales as $e^{-\lambda_n(z_0-z_I)}$ which will dominate every other term for $\lambda_n = O(1)$ and $z_0 - z_I = O(1)$. Thus, to the leading order

$$S \ \sim \ S^0 = \lambda_n^{-1}\beta_3 e^{-\lambda_n(z_0-z_I)}(0,0,1,0,0,0,0) \tag{C19}$$

Here we comment that even if we were not to ignore the contribution to S_l for $l \geq 5$ on the grounds that $z_0 - z_I$ is large and therefore $e^{-\lambda_n(z_0-z_I)}$ small, it would not affect our leading order results for Z_1, Z_3 through Z_5 because of the the special structure of the reduced matrix M in this limit. Therefore, the results quoted in (209) and (210) would equally be valid in this case since the contribution of Z_2, Z_6 through Z_8 for interfacial properties $a_n(z_0)$ and $b_n(z_0)$ (given by (199) and (200)) are exponentially small.

Now, consider simplification of the matrix M, whose elements are shown in (189)-(198). We notice that

$$M \ \sim \ M^0 + O(\gamma^{-1}, \gamma^{-5}\lambda_n^2 R_c) \ , \tag{C20}$$

where the only nonzero elements of M^0 are

$$M^0_{k,j} = \omega_j^{k-1} \quad \text{for k} = 1,2 \ \text{j} = 3,4,5 \ , \tag{C21}$$

$$M^0_{3,j} = -\lambda_n^{-1}\omega_j^{-1} \ , \tag{C22}$$

$$M^0_{4,1} = -p_1 - m_1 + m_2 \ , M^0_{4,2} = e^{p_2(z_0-z_2)}\ (-p_2 - m_1 + m_2) \ , M^0_{4,j} = -m_2\omega_j^{-2} \ \text{for j} = 3,4,5 \ , \tag{C23}$$

$$M^0_{5,1} = e^{p_1(z_2-z_0)} \ , \ \ M^0_{5,2} = 1 \ , \ M^0_{5,j} = -\omega_j^{-2} \ \text{for j} = 6,7,8 \ , \tag{C24}$$

$$M_{6,j} = 1 \ \text{ and } \ \text{M}_{7\text{j}} = \omega_\text{j} \quad \text{for j} = 6,7,8 \ , \tag{C25}$$

$$M^0_{8,1} = -e^{p_1(z_2-z_0)} \ , \ \ M^0_{8,2} = -1 \ . \tag{C26}$$

The solution to

$$M^0 Z^0 = S^0 \tag{C27}$$

can be found in closed form. We find $(Z_6^0, Z_7^0, Z_8^0) = (0,0,0)$,

$$(Z_3^0, Z_4^0, Z_5^0) = \left(-\frac{1}{2} + i\frac{\sqrt{3}}{6}, 1, -\frac{1}{2} - i\frac{\sqrt{3}}{6}\right) \beta_3 e^{-\lambda_n(z_0 - z_I)}. \qquad (C28)$$

Once this is found, it is clear that

$$(Z_1^0, Z_2^0) = -\frac{2m_2\beta_3 e^{-\lambda_n(z_0 - z_I)}}{(p_1 + m_1 - m_2) - e^{(p_1 - p_2)(z_2 - z_0)}(p_2 + m_1 - m_2))} \left(1, -e^{p_1(z_2 - z_0)}\right). \qquad (C29)$$

Figure and Table Captions

Figure 1: Schematic diagram of the Bridgman apparatus.

Table 1: Nomenclature. Note all listed variables are non-dimensionalized.

Table 2: Relation of non-standard symbols with more common notation in Literature.

Table 1: Nomenclature

T	Nondimensional temperature, $\frac{\tilde{T}-\tilde{T}_0}{\tilde{T}_2-\tilde{T}_0}$ where $\tilde{T}$: temp.; $\tilde{T}_0$: planar interfacial temp for pure material and $\tilde{T}_2$: top temperature.
c	relative concentration of one binary component
$\vec{v}=(u,w)$	Fluid velocity relative to velocity of container. u and w: radial and axial components
z	$\frac{\tilde{z}-\tilde{z}_1}{a}$, where $\tilde{z}$: axial coordinate and $\tilde{z}_1$: $\tilde{z}$ at the lower cylinder end.
z_I	Value of z at the lower end of the insulation zone in Fig. 1
z_{II}	Value of z at the upper end of the insulation zone in Fig. 1
z_0	Value of z at the unperturbed interface
z_2	Value of z at the cylinder top in Fig. 1
r	$\frac{\tilde{r}}{a}$, where $\tilde{r}$: radial coordinate.
α	Nondimensional thermal expansion: $\alpha=\tilde{\alpha}(\tilde{T}_2-\tilde{T}_0)$, where $\tilde{\alpha}$: volumetric thermal expansion coefficient.
β	Coefficient of volumetric expansion due to increase in c
ν	Actual Viscosity$/(aU_a)$, where a: cylinder radius, U_a container velocity.
κ	Thermal diffusivity in the melt $/(aU_a)$
D	solutal diffusivity in the melt $/(aU_a)$
κ_s	Thermal diffusivity in the solid $/(aU_a)$
D_s	solutal diffusivity in the solid $/(aU_a)$
ϵq_1	Biot number related to horizontal heat transfer on the melt side , where $\epsilon << 1$ is chosen so that $q_1 = O(1)$
ϵq_{1_s}	Biot number related to horizontal heat transfer on the solid side , where $\epsilon << 1$ is chosen so that $q_{1_s} = O(1)$
ϵq_2	Nusselt number related to horizontal heat transfer on the melt side
ϵq_{2_s}	Nusselt number related to horizontal heat transfer on the solid side
c_2	Concentration at the cylinder top
k	Seggregation coefficient
p	$\frac{\text{Fluid pressure}}{\rho_0 U_a^2}$, where ρ_0: density at temperature $\tilde{T}_0$ and concentration c_2
g	acceleration due to gravity $\times\ a/U_a^2$
S_t	Stefan number: $\frac{\text{Latent Heat}}{(\tilde{T}_2-\tilde{T}_0)c_p}$
d_0	surface tension/(Latent heat $\times$ a)
m	Slope of liquidus line $\times$ $(\tilde{T}_2-\tilde{T}_0)$
R_T	Thermal Rayleigh Number $\frac{g\alpha T^{0'}}{\kappa\nu}$ where $T^{0'}$: z derivative of T^0, the unperturbed T corresponding to $\epsilon=0$
R_c	Solutal Rayleigh Number $\frac{g\beta}{D\nu}\left(\frac{c_i^0-c_2}{1-e^{-(z_2-z_0)/D}}\right)$ where c_i^0: interfacial concentration of $\epsilon=0$ state
$h(z)$	Convenient symbol for $e^{-\frac{z-z_0}{D}}$
λ_n	nth positive zero of Bessel function J_1
γ	Convenient symbol for $[\lambda_n^2 R_T]^{1/6}$

Table 1: Nomenclature. Note all listed variables are non-dimensionalized.

Table 2: Relation of non-standard with standard parameters in Literature

D	$= Pe^{-1}$, where Pe: Peclet number	$D^{-1} << R_T^{1/6}$.
D_s	$= (D_s/D)Pe^{-1}$, where D_s/D: Ratio of solid to melt solute diffusivity	No restriction .
ν	$= Re^{-1}$, where Re: Reynolds number based on translation rate U_a .	$Re << R_T^{1/6}$.
z_2	$= A^{-1}$, where A: Ratio between cylinder radius and length.	No restriction.
κ	$= Re^{-1}Pr^{-1}$, where Pr = Prandtl number	$\kappa/z_2 >> 1$.
κ_s	$= (\kappa_s/\kappa)Re^{-1}Pr^{-1}$, where κ_s/κ: Ratio of solid and melt heat diffusivity.	$\kappa_s/z_2 >> 1$.
R_T	Thermal Rayleigh Number $\frac{\tilde{g}\tilde{\alpha}\frac{d\tilde{T}^0}{d\tilde{r}}a^4}{\tilde{\kappa}\tilde{\nu}}$, where $\tilde{}$ denotes dimensional quantities, $\tilde{T}^0$: Limiting linear Temp. profile of Tiller et al (1953) for $\kappa/z_2 >> 1$.	$R_T >> 1$.
R_c	Solutal Rayleigh number $\frac{\tilde{g}\beta(c_i-c_2)a^3}{\tilde{D}\tilde{\nu}(1-e^{-(z_2-z_0)Pe})}$, where c_i: Tiller et al (1953) interface concentration.	$\lvert R_c\rvert << R_T^{5/6}$.
$g\alpha$	$= R_T Re^{-2}Pr^{-1}\Lambda^{-1}$, where $\Lambda = \frac{a\frac{dT^0}{dr}}{(T_2-T_0)}$.	No expl. restr.
$g\beta$	$= R_T Re^{-1}Pe^{-1}(c_i-c_2)^{-1}\Delta^{-1}$, $\Delta = 1-e^{-Pe(z_2-z_0)}$	No expl. restr.

Table 2: Relation of non-standard symbols with more common notation in Literature.

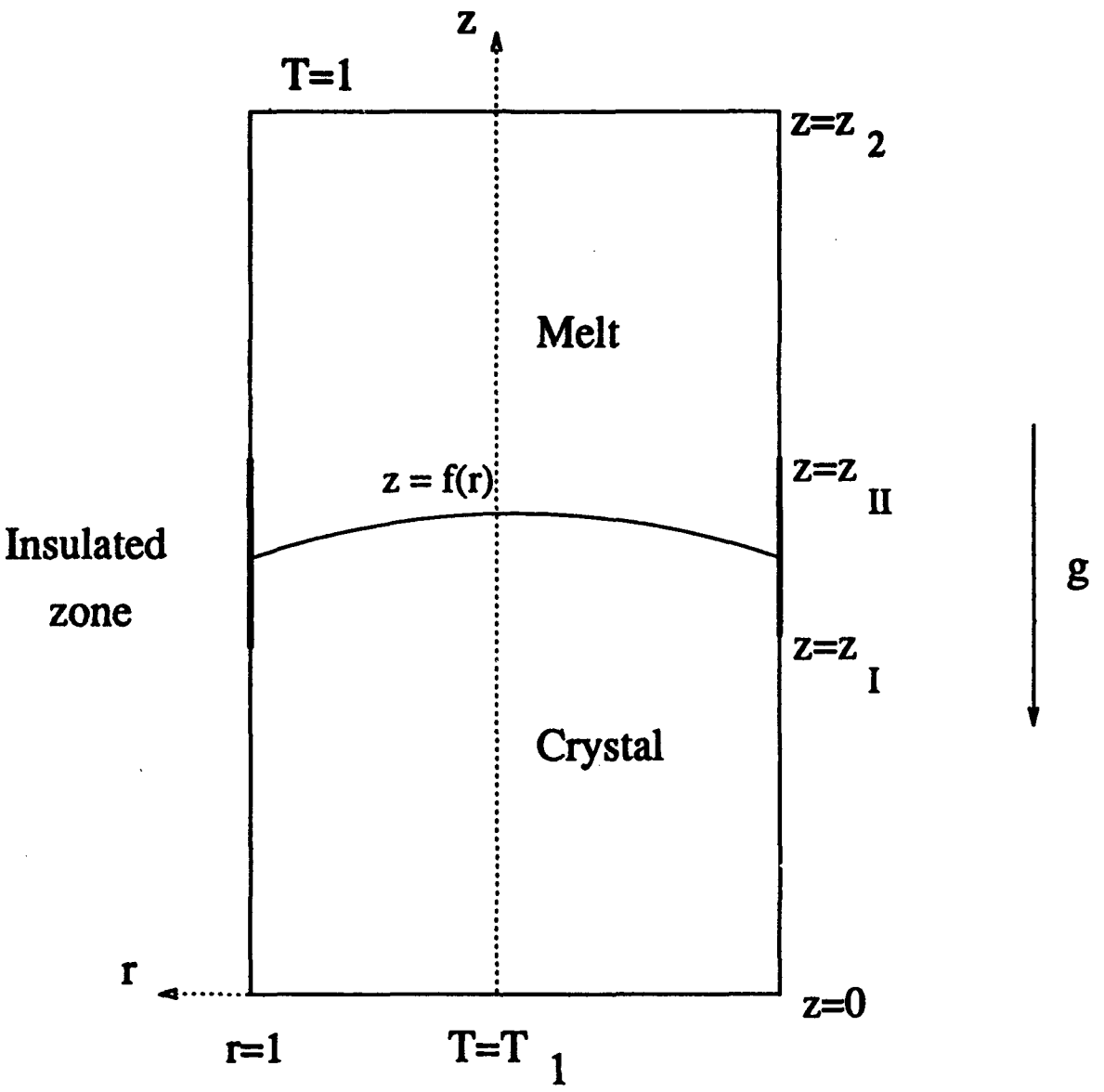

Figure 1: Schematic diagram of the Bridgman apparatus.

REPORT DOCUMENTATION PAGE

Form Approved
OMB No. 0704-0188

1. AGENCY USE ONLY (Leave blank)	2. REPORT DATE	3. REPORT TYPE AND DATES COVERED
	September 1993	Contractor Report

4. TITLE AND SUBTITLE
CONVECTION EFFECTS ON RADIAL SEGREGATION AND CRYSTAL MELT INTERFACE IN VERTICAL BRIDGMAN GROWTH

5. FUNDING NUMBERS
C NAS1-18605
C NAS1-19480
WU 505-90-52-01

6. AUTHOR(S)
S. Tanveer

7. PERFORMING ORGANIZATION NAME(S) AND ADDRESS(ES)
Institute for Computer Applications in Science and Engineering
Mail Stop 132C, NASA Langley Research Center
Hampton, VA 23681-0001

8. PERFORMING ORGANIZATION REPORT NUMBER
ICASE Report No. 93-72

9. SPONSORING/MONITORING AGENCY NAME(S) AND ADDRESS(ES)
National Aeronautics and Space Administration
Langley Research Center
Hampton, VA 23681-0001

10. SPONSORING/MONITORING AGENCY REPORT NUMBER
NASA CR-191541
ICASE Report No. 93-72

11. SUPPLEMENTARY NOTES
Langley Technical Monitor: Michael F. Card
Final Report
Submitted to Physics of Fluids A

12a. DISTRIBUTION/AVAILABILITY STATEMENT
Unclassified - Unlimited

Subject Category 34

12b. DISTRIBUTION CODE

13. ABSTRACT (Maximum 200 words)
We analytically study the influence of convection caused by horizontal heat transfer through the sides of a vertical Bridgman apparatus. We consider the case when the heat transfer across the side walls is small so that the resulting interfacial deformation and fluid velocities are also small. This allows us to linearize the Navier-Stokes equations and express the interfacial conditions about a planar interface through a Taylor expansion. Using a no tangential stress conditions on the side walls, asymptotic expressions for both the interfacial slope and radial segregation at the crystal-melt interface are obtained in closed form in the limit of large thermal Rayleigh number. It is suggested that these can be reduced by appropriately controlling a specific heat transfer property at the edge of the insulation zone in the solid side.

14. SUBJECT TERMS
crystal growth; convection effects; Bridgman apparatus

15. NUMBER OF PAGES
58

16. PRICE CODE
A04

17. SECURITY CLASSIFICATION OF REPORT	18. SECURITY CLASSIFICATION OF THIS PAGE	19. SECURITY CLASSIFICATION OF ABSTRACT	20. LIMITATION OF ABSTRACT
Unclassified	Unclassified		

NSN 7540-01-280-5500

Standard Form 298 (Rev. 2-89)
Prescribed by ANSI Std Z39-18
298-102

☆U.S. GOVERNMENT PRINTING OFFICE: 1993 - 528-064/86075